Acta Geodyn. Geomater., Vol. 22, No. 1 (217), 65–86, 2025
DOI: 10.13168/AGG.2025.0006
journal homepage: https://www.irsm.cas.cz/acta

ORIGINAL PAPER

CRUSTAL ANISOTROPY, MOHO AND CONRAD DEPTHS, AND TOPOGRAPHY OF THE 410 AND 660 KM DISCONTINUITIES BENEATH MALAYSIA, MYANMAR, AND THAILAND REVEALED BY P-WAVE RECEIVER FUNCTIONS AND COMMON CONVERSION POINT STACKING

Kasemsak SAETANG [1)] * and Wilaiwan SRISAWAT [2)]

[1)] *Program in Physics, Faculty of Education, Nakhon Si Thammarat Rajabhat University, Nakhon Si Thammarat, 80280, Thailand*
[2)] *Science and Technology Unit, Watthapho Municipal School, Nakhon Si Thammarat, 80000, Thailand*

**Corresponding author's e-mail:* light2529@gmail.com

ARTICLE INFO

Article history:
Received 14 February 2025
Accepted 17 March 2025
Available online 25 March 2025

Keywords:
Crustal anisotropy
Moho and Conrad discontinuities
Common Conversion Point (CCP) stacking
410 km and 660 km discontinuities
Receiver function
Southeast Asia tectonics

ABSTRACT

This study utilizes advanced seismic methods to investigate the complex geodynamic processes beneath the West Burma, Shan-Thai, Indo-China terranes, and the Gulf regions of Southeast Asia. Through the comprehensive analysis of teleseismic waveforms from 25 seismic stations across Malaysia, Myanmar, and Thailand, crustal anisotropy and the depths of the Conrad and Moho discontinuities are investigated, while also mapping the topography of the mantle transition zone (MTZ) discontinuities at 410 and 660 km. Utilizing H-K stacking and Common Conversion Point (CCP) stacking, this study provides detailed estimations of crustal thickness (H) and Vp/Vs ratios (k), highlighting significant crustal thickening in the West Burma Terrane consistent with subduction processes beneath the Sunda megathrust. The gradual increase in Moho depth within the Shan-Thai Terrane towards the Indo-China Terrane boundary, alongside Conrad discontinuity variations, underscores its complex tectonic evolution. In contrast, the Indo-China Terrane exhibits pronounced crustal thickening, reflective of its intricate collisional history. Additionally, observations in the Gulf regions indicate shallower crustal thickness and evidence of mantle upwelling, with implications for seismic risk assessment and geodynamic modeling in Southeast Asia.

1. INTRODUCTION

The lithosphere, which includes Earth's crust and upper mantle, constitutes a pivotal component in the study of geodynamics. Its analysis is integral to determining Earth's geological evolution, governed by internal thermodynamics and external solar influences. Despite its significance, our comprehension of the lithosphere is often hampered by the paucity of the geological record and the inherent challenges in deep subsurface exploration (Hawkesworth et al., 2017). To identify the evolutionary trajectory of the lithosphere, it is imperative to scrutinize the cyclical processes of lithogenesis and subsequent geological modifications. This examination reveals the intricate interplay among various geospheric systems, which is crucial for understanding tectonic activities and geodynamic phenomena, particularly during epochs of supercontinental amalgamation and disintegration (Hawkesworth et al., 2017).

Within the Southeast Asian context, the crustal anisotropy and mantle discontinuities beneath Malaysia, Myanmar, and Thailand provide a unique window into the region's complex tectonic framework. Myanmar's geological history during the Cretaceous period is marked by low-angle extensional faulting in the Mogok Belt, leading to significant subsidence in the Eastern and Western troughs (Than et al., 2017). This tectonic activity progressed into the Middle to Late Cenozoic, as evidenced by the formation of the Moza Formation and the Khabo Sandstone (Than et al., 2017). Furthermore, the Irrawaddy Formation, with its distinctive fluvial architecture, underscores the region's tectonic history of sedimentation and tectonic processes (Than et al., 2017).

Thailand is located at the northern boundary of Sundaland and consists of terranes that have undergone significant tectonic reconfiguration since the late Paleozoic (Morley et al., 2011). This intricate tectonic mosaic, distinguished by variegated structural expressions, accentuates the seismic vulnerability of the region. Despite extensive geological documentation, integrated geophysical studies remain limited, particularly those addressing the profound structural and seismic configurations of Thailand (Cobbing, 2011; Hansen and Wemmer, 2011; Ridd et al., 2011; Searle and Morley, 2011).

The confluence of these geological events in Southeast Asia, particularly with respect to crustal anisotropy and mantle discontinuities, highlights the necessity of conducting rigorous geophysical research. This study, therefore, employs advanced seismic methodologies to dissect the complexities surrounding the Mohorovičić (Moho) and Conrad discontinuities,

Cite this article as: Saetng K, Srisawat W: Crustal anisotropy, Moho and Conrad depths, and topography of the 410 and 660 km discontinuities beneath Malaysia, Myanmar, and Thailand revealed by P-wave receiver functions and common conversion point stacking. Acta Geodyn. Geomater., 22, No. 1 (217), 65–86, 2025. DOI: 10.13168/AGG.2025.0006

alongside the 410 and 660 km mantle discontinuities. These efforts are geared towards enhancing our understanding of lithospheric and mantle dynamics in this tectonically active region, contributing significantly to the global geophysical discourse.

In situating our research within the broader scope of global geophysics, it is imperative to recognise concomitant advancements in Receiver Functions and Common Conversion Point (CCP) Stacking methodologies. For example, CCP Stacking was deployed in northern Australia by Sun and Kennett (2020), while Guan and Niu (2017) refined this method in northeast China. These studies furnish a comparative framework for our analysis, accentuating the universal applicability of our methodology. Contemporary research within Myanmar and the Malay Peninsula, inclusive of southern Thailand, has illuminated crustal attributes and thickness variances (Latiff and Khalil, 2019; Nwe et al., 2022), demonstrating significant regional disparities that enhance our comprehension of the area's geological heterogeneity and complexity. Previous investigations of crustal structure beneath the Malaysian peninsula have determined crucial lithospheric properties that inform regional tectonic interpretation. Latiff and Khalil (2019) implemented joint inversion of receiver functions and surface wave dispersion to determine that the Moho discontinuity beneath Peninsular Malaysia occurs at depths of 24-32 km with corresponding Vp/Vs ratios of 1.73-1.79. Their analysis further delineated Conrad discontinuity depths predominantly between 10-13 km across the peninsula.

The demarcation between the Shan-Thai and Indo-China Terranes within the confines of Thailand, bifurcated by a Late Jurassic suture (Stokes et al., 1996) as depicted in Figure 1, encapsulates a record of significant geologic evolution. To the west of this boundary, the West Burma Terrane (WBT) adjoins the Shan-Thai Terrane and extends into Myanmar, forming an integral part of the Southeast Asian tectonic fabric. Within this intricate tectonic mosaic, the Western Highlands of Thailand, also termed the Tenasserim Hills or Tanintharyi Hills (Ridd, 2017), emerge as a geologically significant entity. Extending from the northern end of the Thai-Malay Peninsula down to the Isthmus of Kra, this region, which is part of the ancient Sunda Shelf, is typified by its venerable and highly metamorphosed rocks, predominantly granitic, shaped by extensive tectonic activities such as subduction, collision, and accretion throughout the Paleozoic and Mesozoic eras.

Adding to this complex tectonic framework, the Mergui Group of the Karen–Tenasserim Unit extensively crops out in southern Myanmar and extends eastwards into Thailand, where it is known as the Phuket Group or the Kaeng Krachan Formation. Its considerable thickness and structural complexity, as evidenced by its extensive areal extent and the absence of marker beds, suggest a rich geological history. The unit's continuation into Thailand is delineated by the Khlong Marui Fault, a significant tectonic discontinuity that highlights the distinct Paleozoic successions on either side of the fault. This geological fabric, undergoing significant folding and faulting, contributes to our understanding of a region formed by complex geological processes (Ridd, 2017).

The central basin of Thailand, rich in complex geological characteristics, exemplifies a dynamic tectonic history shaped by varied geological processes. This region has experienced significant tectonic evolution marked by rift activities, evident in the diverse timing of rifting across basins, such as the early rifting in the Mae Lamao and Mae Chaem basins and the Middle Miocene origins of the Mae Moh basin. Accompanying this tectonic activity are varied patterns of basin subsidence and sedimentation, with notable subsidence in the Suphan Buri basin during the Pliocene and the Phitsanulok basin in the Middle Miocene. The structural complexity of the region is highlighted by features like the Mae Ping fault zone, exhibiting both early ductile left-lateral motion and later brittle right-lateral motion. Thermal subsidence, particularly during the Pliocene, is evident in the formation of thermal subsidence basins, correlating with low crustal temperatures. The evolution of these basins displays diachronous patterns, suggesting diverse end points to rifting, and has been influenced by varied inversion episodes and stress regimes, primarily oriented NW-SE to NE-SW. This intricate geological landscape, characterized by the interplay of extensional, compressional, and strike-slip forces alongside thermal and sedimentary processes, defies simple tectonic models, reflecting the complex and multifaceted nature of basin evolution in this tectonically active area (Morley et al., 2001).

The Khorat Plateau, a vital component of the Indochina Terrane in northeastern Thailand, exhibits a multifaceted geological composition and stratigraphy. It is primarily characterized by the Mesozoic Khorat Group (Singtuen et al., 2023), encompassing formations like Phra Wihan, Sao Khua, Phu Phan, and Khok Kruat, which are predominantly composed of red-bedded sedimentary rocks—sandstone, siltstone, shale, and pebble sandstone—alongside calcrete, rock salt, gypsum, and anhydrite. These sedimentary rocks, mainly sandstones and shales, were deposited in a vast basin during the Jurassic and Cretaceous periods. The plateau's geological evolution has been profoundly influenced by the Indosinian orogeny, stemming from the collision between the Indochina and Sibumasu Terranes in the late Triassic, leading to uplift movements, tectonic faulting, and the formation of inter-mountain thermal sag basins filled with continental sediments. The plateau's topography, predominantly flat and gently undulating with altitudes between 100 and 200 meters above sea level (Rattana, 2020), is shaped by tectonic uplift and erosion. The plateau is also notable for its paleontological significance, marked as the site of Thailand's first dinosaur fossil excavation, and for the

discovery of diverse dinosaur species. Furthermore, its extensive deposits of potash and rock salt, remnants of ancient evaporite formations, coupled with its geological history closely tied to the tectonic movements of the Indochina Block (Minezaki et al., 2009) and the broader geodynamic processes of the Southeast Asian region, render the Khorat Plateau a region of significant geoscientific interest, especially for understanding its complex structural and stratigraphic dynamics.

Recent seismological investigations in Thailand, utilizing advanced techniques like body-wave travel-time tomography and focal mechanism analysis, have substantially improved our understanding of the regional crustal structures and seismic dynamics. References such as Noisagool et al., 2014, 2016; Pananont et al., 2017; Saetang, 2017, 2022; Saetang et al., 2018 and Saetang and Duerrast, 2023 highlight the evolving knowledge in this field. These studies, considering the intricacies of the West-Burma Terrane (WBT), offer an enhanced view of the seismic landscape, crucial for seismic risk assessments in this tectonically complex area.

Moreover, the application of a two-layer model for shear-wave splitting analysis (Saetang, 2022) has provided a deeper insight into the anisotropy patterns beneath Myanmar and Thailand. This approach revealed that the splitting observations align better with a two-layer model, comprising lithospheric and asthenospheric flows, than with a single-layer model. Particularly noteworthy are the distinct flow directions in the lithosphere and asthenosphere, and the weaker anisotropy in the West-Burma Terrane compared to the Shan-Thai Terrane, which underscores the significant differences in seismic behaviors and tectonic processes between these terranes.

Additionally, an in-depth analysis of the focal mechanisms of Mw 6.3 aftershocks in the Phayao Fault Zone (Saetang, 2017), as detailed in a recent study, has identified the prevalence of left-lateral strike-slip motion with a reverse component in the northern part of the PFZ, offering valuable insights into the seismic and tectonic behavior in Northern Thailand. Furthermore, tele-seismic receiver function studies across Thailand (Noisagool et al., 2014) have determined variations in crustal thickness and composition, with a gradual increase in crustal thickness from the Shan-Thai terrane to the Khorat Plateau, and corresponding changes in Vp/Vs and Poisson's ratios, indicating a variation in crustal composition that reflects the region's complex tectonic history.

Building upon this foundation, the research by Charusiri et al. (1993) identifies the geological intricacies of Thailand's granitic belts through 40Ar/39Ar geochronological analysis, delineating a protracted history characterized by diverse mineralizations and geotectonic environments across the Eastern, Central, and Western Granite Belts as illustrated in Figure 1. These granitoids, linked with mineral deposits such as tin, tungsten, and rare earth elements, form a longitudinal mountain chain traversing north to south Thailand, each segment delineated by distinct geological environments, rock types, distributions, ages, and associated mineral deposits. The comprehensive characterization of the granitoid belts significantly propels our understanding of the regional geotectonic evolution and bears critical implications for mineral exploration.

Figure 2 exemplifies cartographic precision in delineating the tectonic assemblages of the Indo-China (ICT), Shan-Thai (STT), and West-Burma (WBT) terranes, aligning with the geological syntheses of Charusiri et al (1993). This figure integrates seismic lineaments across Malaysia, Myanmar, and Thailand, correlating these with lithospheric kinematic patterns as indicated by GPS velocity vectors. These vectors, derived from comprehensive compilations by Kreemer et al. (2014), Maurin et al. (2010), Simons et al. (2007) and UNAVCO (2021), highlight the relative plate motions.

In the southern part of Thailand, the cartography distinctly annotates the Ranong and Khlong Marui Fault Zones, oriented in Northeast-Southwest directions, as documented by the Department of Mineral Resources (DMR, 2007). This orientation reflects the regional tectonic regime and stress field. To the north, the Mae Hong Son Fault Zone is delineated with a North-South orientation, possibly relating to collisional forces in the northern region. In the western part of Thailand, the Mae Ping and Three Pagodas Fault Zones, oriented in Northwest-Southeast directions, align with the prevailing tectonic fabric.

Within Myanmar, the Sagaing Fault Zone, oriented in a North-South direction, marks a geologically significant boundary that demarcates the division between the West Burma Terrane and the Shan-Thai Terrane. This fault zone is crucial for understanding the seismic and tectonic evolution of the area.

The GPS velocity vectors, quantified in millimetres per annum and depicted by grey arrows, indicate the kinematics of the tectonic plates. Vectors within the West Burma Terrane suggest a relative northward motion, while those within the Shan-Thai Terrane indicate an eastward movement. In the Indo-China Terrane, the vectors are oriented in an east-southeastward direction, denoting complex tectonic interactions with adjacent terranes.

Moreover, the delineation of crustal anisotropy results, illustrated as blue lines on the map, will be comprehensively discussed in the results and discussions section. This discussion will indicate their significance in contributing to the understanding of the tectonic and seismic dynamics within the region, thus enhancing the depth of seismic analysis in this study. Furthermore, recent work by Yu et al. (2018) has made notable contributions in understanding the seismic anisotropy in the Indochina Peninsula. Their analysis of shear wave splitting measurements across 29 stations revealed a dominant east-west fast orientation in the upper mantle anisotropy beneath most of the

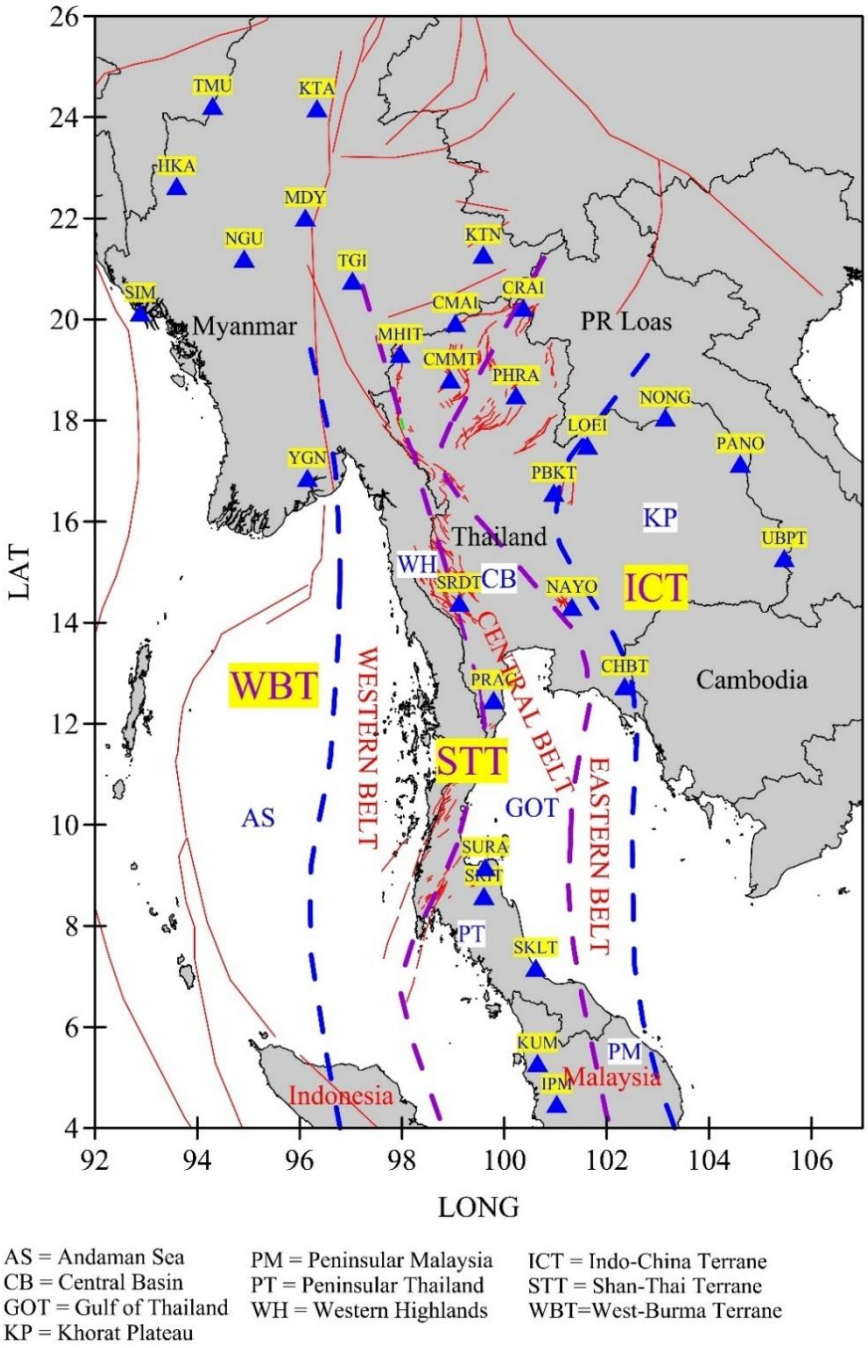

Fig. 1 Tectonic Map of the study area. Depicts key geological terranes and tectonic features in Malaysia, Myanmar, and Thailand, highlighting fault lines and distinguishing the West-Burma, Shan-Thai, and Indo-China Terranes (Charusiri et al., 1993; DMR, 2007; Morley et al., 2011). Blue triangles mark seismic stations, indicating the spatial coverage of the data collection.

peninsula. This finding contrasts with the north-south orientation observed on the southeastern Tibetan Plateau and suggests minimal influence from lithospheric fabrics. The study posits that the anisotropy may be a result of absolute plate motion or westward rollback of the subducted Indian slab, highlighting the complex interplay of tectonic forces in the region. The research by Yu et al. (2018) thus adds a critical dimension to our understanding of mantle dynamics in Southeast Asia, complementing the broader narrative of tectonic and seismic investigations in the region.

2. DATA AND METHODS

Seismic investigations were conducted to scrutinise the intricate crustal and mantle structures beneath Malaysia, Myanmar, and Thailand. These regions are characterised by the convergence of significant tectonic plates. Our primary focus is on the Mantle Transition Zone (MTZ) and the crustal

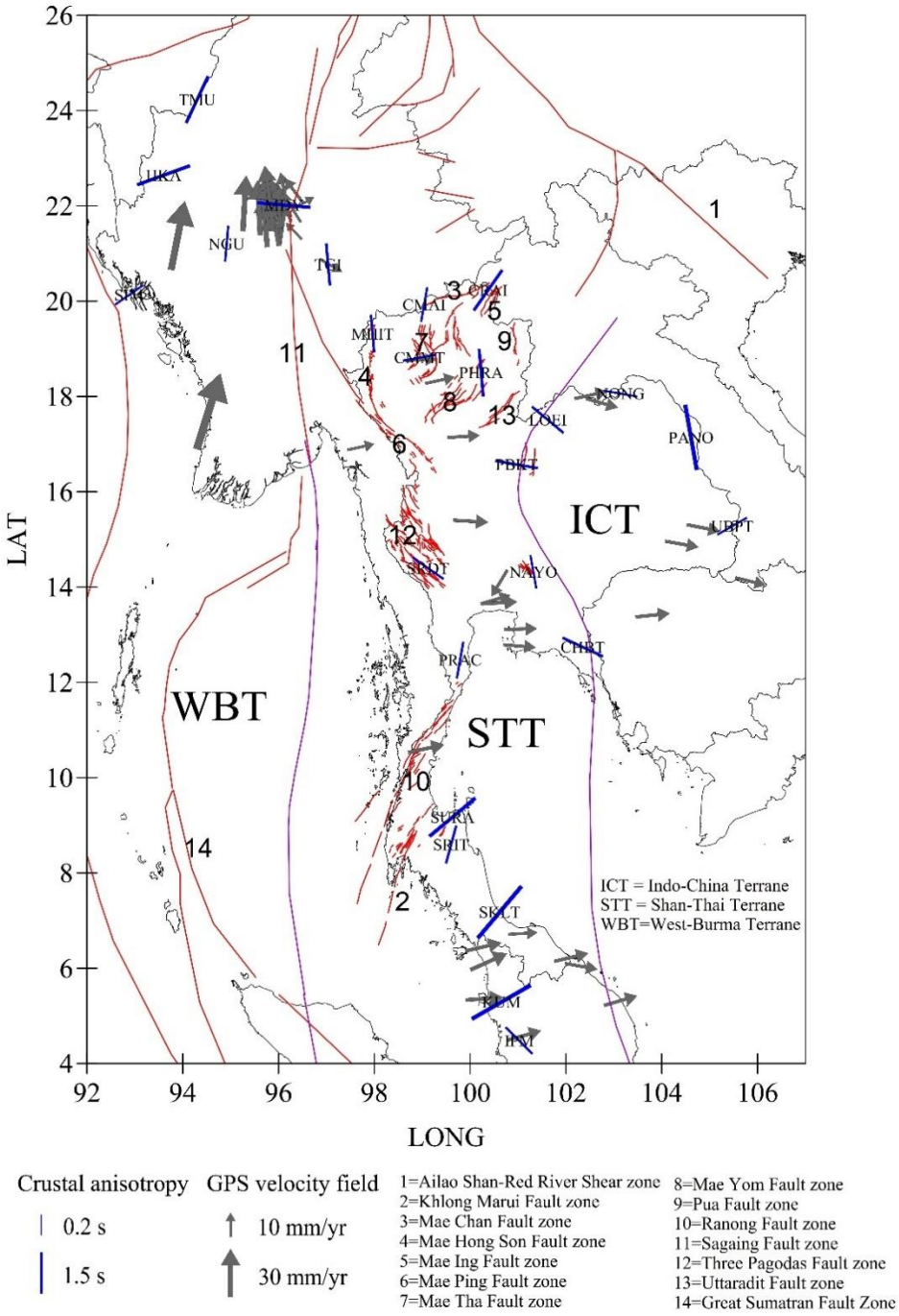

Fig. 2 Tectonic map of Malaysia, Myanmar, and Thailand, illustrating crustal anisotropy with blue lines from this study (with ϕ and δt values in Table 1), major fault lines in red, and GPS velocity vectors in grey. This map provides a clear representation of the tectonic dynamics within the Indo-China Terrane (ICT), Shan-Thai Terrane (STT), and West-Burma Terrane (WBT) (Charusiri et al., 1993; DMR, 2007; Kreemer et al., 2014; Maurin et al., 2010; Morley et al., 2011; Simons et al., 2007; UNAVCO, 2021).

discontinuities, specifically the Mohorovičić (Moho) and Conrad discontinuities, with a particular emphasis on the seismic discontinuities at depths of 410 km and 660 km within the MTZ. To achieve a comprehensive understanding of the crustal structure, including the depths of the Moho and Conrad discontinuities, we employ P-wave Receiver Functions (PRFs) and Common Conversion Point (CCP) Stacking techniques. These techniques are pivotal in analysing teleseismic waveforms recorded by permanent seismic stations, specifically focusing on the P-wave components. Our approach is designed to show new insights into the tectonic processes and crustal composition of these geologically dynamic areas.

The PRFs technique utilizes teleseismic P-waves that generate S-wave conversions (Ps phases) at velocity interfaces. The time delay between direct P-arrivals and these converted phases correlates with discontinuity depths and velocity structures. The CCP stacking methodology enhances signal resolution by

projecting and summing receiver functions at their theoretical conversion points within discretised subsurface volumes, thereby accommodating complex wave propagation geometries and improving the detection of structural features that might remain obscured in individual receiver functions.

For the processing of PRFs, CCP, and crustal anisotropic estimation, we utilised Seispy (Xu and He, 2023), a Python module with a graphical user interface. We acquired teleseismic earthquake waveforms from online catalogues, spanning the operational period of the stations until December 31, 2022. These were sourced via the International Federation of Digital Seismograph Networks (FDSN) web service, provided by the Incorporated Research Institutions for Seismology (IRIS). The selected waveforms were within 30º to 90º epicentral distances and had magnitudes exceeding 5.8. To enhance data quality, linear and mean trends were removed, and a band-pass filter from 0.05 Hz to 2 Hz was applied to reduce coherent noise. The P-wave arrival times for each event were automatically computed using the TauP (Crotwell et al., 1999) submodule in Obspy (Beyreuther et al., 2010), employing the IASP91 velocity model (Kennett and Engdahl, 1991). The waveforms were then trimmed, encompassing a duration of 10 seconds before and 120 seconds after the P-wave arrival time. The signal-to-noise ratio (SNR) was calculated using the following equation (Xu and He, 2023):

$$SNR = 10\ log_{10}(A_S^2/A_N^2) \quad (1)$$

Here A_s and A_N represent the time series after and before the theoretical P arrival, respectively. Subsequently, manual quality control was conducted using a graphical user interface for further validation of the selected events. The waveforms recorded on north-east-vertical (NEZ) components were rotated to transverse-radial-vertical (TRZ) components. An iterative deconvolution technique in the time domain (Ligorría and Ammon, 1999) was then utilized to compute all PRFs. A graphical user interface was subsequently utilized to manually assess the quality of PRFs, rejecting those of inferior quality. Table 1 presents the number of PRFs for stations that met the quality criteria.

To estimate the Moho depth (H) and the average Vp/Vs ratio (k) beneath the seismic stations in Malaysia, Myanmar, and Thailand, we utilized the H-K stacking technique, as refined by Zhu and Kanamori (2000). This technique utilizes teleseismic receiver functions to accurately determine the crustal thickness and Vp/Vs ratio. The large velocity contrast at the Moho discontinuity enables the conversion of incoming teleseismic P wave energy into SV wave, facilitating the measurement of the time separation between the direct P arrival and the conversion phase. This approach provides precise point measurements at the station, benefiting from the steep incidence angle of the teleseismic P waves (see Fig. 3 for a visual representation).

For our analysis, the range for H was set between 23 km and 41 km, within the H range as approximately defined by visual depth picking post-3D CCP stacking, and for k between 1.4 and 2.3, to encompass the expected variations in crustal properties. An average crustal Vp of 6.21 km/s, as determined by Saetang and Duerrast (2023), was chosen for depth conversion. The weights for stacking were carefully selected to optimize the resolution of the phases: 0.5 for the Ps phase, 0.3 for the PpPs phase, and 0.2 for the combined PpSs+PsPs phases. The stacking algorithm developed by Zhu and Kanamori (2000) transforms time domain waveforms into the depth domain, providing the best estimations for both crustal thickness and Vp/Vs ratio. By stacking receiver functions from various distances and directions, we minimized the effects of lateral structure variation, obtaining an average crustal model with assessable uncertainties based on the flatness of the stacking function at its maximum.

In our study, the estimation of crustal anisotropy parameters, specifically the fast polarization direction (ϕ) and delay time (δt), is meticulously conducted using the joint method implemented in Seispy, as visualized in Figure 4. This method, based on the work of Liu and Niu (2012), combines radial energy maximization with cosine moveout correction and transverse energy minimization, depicted in Figure 4a. We manually adjusted the time window for identifying Pms phases in the radial component, considering variations across different back-azimuths, which are illustrated in Figure 4b. We opted for a customized approach, selecting the window based on the discernibility and clarity of Pms phases evident in the receiver function data (Table 1). This methodology allowed for a more nuanced analysis of the seismic waveforms and enhanced the precision of our anisotropy estimations. The results of this comprehensive anisotropic analysis, including the calculated values of ϕ and δt for each seismic station, are presented in Table 1. This table not only compares the Moho depth (H) and Vp/Vs ratio (k) across various stations but also showcases the crustal anisotropy parameters derived from our integrated approach, thereby bridging our methodology with the observed outcomes.

The importance of this methodology lies in its capability to analyze all receiver functions recorded at a single seismic station jointly, as demonstrated in Figure 4b, where the left panel shows the radial component and the right panel shows the transverse component. This approach is preferred over analyzing individual receiver function data to avoid large errors and potential misestimations of crustal anisotropy. It offers a robust and reliable way to identify and estimate crustal anisotropy, using R receiver functions due to their typically better signal-to-noise ratios (SNRs) compared to T receiver functions. The results of this anisotropic estimation, as detailed in Table 1, are generated automatically after executing the process, showcasing the outcomes of our integrated

Table 1 Mohorovičić (Moho) and Conrad discontinuity depths, Vp/Vs ratios, and crustal anisotropy parameters at seismic monitoring stations across Malaysia, Myanmar, and Thailand.

Station	Latitude	Longitude	Elevation (m)	H-K Stacking from This Paper			H-K Stacking from Previous Works			H (km) from CCP	Conrad depth beneath a station from CCP (km)	Crustal Anisotropy			
				H (km) ± Error	k ± Error	N	H (km) ± Error	k ± Error	N			ϕ (°)	$\delta t(s)$	Pms Phase Search Range (s)	Pms Phase Window Half-Length (s)
CHBT	12.74	102.35	4	38.50 ±0.61	1.730± 0.056	63	28.96 ±0.90 (Noisagool et al. 2014)	1.760± 0.019 (Noisagool et al. 2014)	40 (Noisagool et al. 2014)	38	22	115	0.6	4-6	2
CMAI	19.93	99.04	1533	30.50 ±1.06	1.760± 0.042	80	32.20 ±0.44 (Noisagool et al. 2014)	1.740± 0.012 (Noisagool et al. 2014)	26 (Noisagool et al. 2014)	30	17	10	0.25	3-5	2
CMMT	18.81	98.94	400	30.80 ±0.80	1.670± 0.032	586	32.31 ±0.33 (Noisagool et al. 2014)	1.670± 0.031 (Noisagool et al. 2014)	119 (Noisagool et al. 2014)	26		80	0.20	2-5	2
CRAI	20.23	100.37	357	29.70 ±0.86	1.740± 0.034	230				29		35	0.80	3-5	2
HKA	22.64	93.60	1733	28.70±0.01	1.66± 0.001	471	49.4 (Nwe et al. 2022)	1.83 (Nwe et al. 2022)		25		70	1.05	2-6	3
IPM	4.48	101.02	5	29.00 ±0.48	1.770± 0.026	1369	24-32 (Latiff and Khalil 2019)	1.79 (Latiff and Khalil 2019)	889 (Latiff and Khalil 2019)	29	14	135	0.35	3-5	2
KUM	5.29	100.65	5	32.80 ±0.59	1.710± 0.027	1606	30 (Latiff and Khalil 2019)	1.73 (Latiff and Khalil 2019)	937 (Latiff and Khalil 2019)	28		240	1.50	2-6	3
LOEI	17.51	101.62	306	33.40 ±1.34	1.740± 0.048	146	34.92±1.23 (Noisagool et al. 2014)	1.740± 0.013 (Noisagool et al. 2014)	17 (Noisagool et al. 2014)	32	20	310	0.47	3-6	2
MDY	22.02	96.11	22	27.50 ±1.31	1.77± 0.060	183	35.5 (Nwe et al. 2022)	1.60 (Nwe et al. 2022)		27		275	0.95	2-5	2
MHIT	19.32	97.96	270	32.20 ±0.78	1.710± 0.033	227	34.59±0.24 (Noisagool et al. 2014)	1.67 ± 0.009 (Noisagool et al. 2014)	51 (Noisagool et al. 2014)	30	14	175	0.35	3-5	2
NAYO	14.32	101.32	106	33.20 ±0.76	1.750± 0.030	196	35.18 ±1.70 (Noisagool et al. 2014)	1.700± 0.040 (Noisagool et al. 2014)	33 (Noisagool et al. 2014)	33		170	0.20	2-6	2
NGU	21.21	94.92	21	35.40 ±0.86	1.890± 0.024	384	34.5 (Nwe et al. 2022)	1.94 (Nwe et al. 2022)		32	12	5	0.28	3-7	3
NONG	18.06	103.14	140	36.90 ±0.94	1.750± 0.029	277	39.28±0.42 (Noisagool et al. 2014)	1.710± 0.014 (Noisagool et al. 2014)	30 (Noisagool et al. 2014)	38		100	0.20	3-6	3
PANO	17.14	104.61	136	40.30 ±1.70	1.680± 0.063	24				37	16	350	1.45	3-6	3
PBKT	16.57	100.97	8	37.90 ±0.81	1.680± 0.028	154	40.03 ±0.24 (Noisagool et al. 2014)	1.670± 0.007 (Noisagool et al. 2014)	96 (Noisagool et al. 2014)	34		100	0.55	3-6	2
PHRA	18.50	100.23	187	31.60 ±1.04	1.730± 0.051	108				30	17	175	0.73	3-5	2
PRAC	12.47	99.79	54	28.20 ±0.61	1.690± 0.026	374	30.04 ±0.45 (Noisagool et al. 2014)	1.660± 0.011 (Noisagool et al. 2014)	26 (Noisagool et al. 2014)	25		10	0.33	2-4	2
SIM	20.13	92.88	20	26.20 ±0.64	1.470± 0.032	189	26.0 (Nwe et al. 2022)	1.50 (Nwe et al. 2022)		29	16	55	0.2	1-3	2

Table 1 continued

Station	Latitude	Longitude	Elevation (m)	H-K Stacking from This Paper			H-K Stacking from Previous Works			H (km) from CCP	Conrad depth beneath a station from CCP (km)	Crustal Anisotropy			
				H (km) ± Error	k ± Error	N	H (km) ± Error	k ± Error	N			ϕ (°)	$\delta t(s)$	Pms Phase Search Range (s)	Pms Phase Window Half-Length (s)
SKLT	7.18	100.62	14	26.10 ±0.67	1.670± 0.031	335	27.44±0.25 (Noisagool et al. 2014)	1.670± 0.009 (Noisagool et al. 2014)	47 (Noisagool et al. 2014)			220	1.50	2-4	2
SRDT	14.40	99.12	122	28.80 ±0.68	1.690± 0.027	504	29.74±0.53 (Noisagool et al. 2014)	1.680± 0.016 (Noisagool et al. 2014)	46 (Noisagool et al. 2014)	26		125	0.35	3-5	2
SRIT	8.60	99.60	58	31.40 ±0.55	1.650± 0.025	344	28 (Latiff and Khalil 2019)	1.77 (Latiff and Khalil 2019)	278 (Latiff and Khalil 2019)	26	11	15	0.4	2-5	2
SURA	9.17	99.63	-5	27.90 ±1.02	1.810± 0.064	135	28 (Latiff and Khalil 2019)	1.72 (Latiff and Khalil 2019)	314 (Latiff and Khalil 2019)	33	15	230	1.2	2-5	2
TGI	20.77	97.03	21	40.50 ±1.02	1.690± 0.027	495	33 (Nwe et al. 2022)	1.84 (Nwe et al. 2022)		38		175	0.53	3-6	2
TMU	24.23	94.30	24	40.50 ±0.06	2.203± 0.002	507	50.5 (Nwe et al. 2022)	1.99 (Nwe et al. 2022)		35		25	0.88	3-6	2
UBPT	15.28	105.47	120	35.60 ±2.69	1.750± 0.066	275	33.67±2.76 (Noisagool et al. 2014)	1.790± 0.060 (Noisagool et al. 2014)	26 (Noisagool et al. 2014)	35	11	60	0.2	3-6	2

anisotropic analysis using Seispy. This table compares the Moho depth (H), Vp/Vs ratio (k), and crustal anisotropy parameters for each seismic station from our current study with those from previous works.

A distinctive feature of this methodology is the joint analysis of all receiver functions recorded at a single seismic station, preferred over analyzing individual receiver function data to avoid large errors and potential misestimations of crustal anisotropy. The method proposes three different ways to estimate seismic anisotropy, focusing on using R receiver functions due to their typically better signal-to-noise ratios (SNRs) compared to T receiver functions. The first method searches for parameters that maximize the stacked Ps amplitude after a cosine moveout correction in the Ps arrival time. The second and third methods involve a full correction of seismic anisotropy on R and T receiver functions, tracking the effects of the correction on the R cc and T energy, respectively. The minimization of T energy is found to better recover input models, although it can misinterpret structures like a dipping Moho with crustal anisotropy when backazimuth coverage is poor.

The results of this anisotropic estimation are generated automatically after executing the process, ensuring a comprehensive and efficient analysis. This integrated technique, combining individual and joint measurements of seismic anisotropy along with SNRT analysis, provides a robust and reliable way for identifying and estimating crustal anisotropy with receiver function data.

This study employs the Seispy software (Xu and He, 2023) to address significant depth errors associated with traditional time-to-depth conversion methods, especially relevant for deep discontinuities such as the 410 and 660 km discontinuities. Conventionally, the ray parameters of converted phases, like Ps or Sp, are approximated as those of direct phases, which can lead to considerable inaccuracies in depth determination (Shi et al., 2020). To mitigate this issue, the analysis employs the TauPy submodule in Obspy (Crotwell et al., 1999; Beyreuther et al., 2010) through the Seispy software (Xu and He, 2023), leveraging both the IASP91 1D velocity model (Kennett and Engdahl, 1991) and the GyPSuM 3D velocity model (Simmons et al., 2010). These models enable us to calculate the ray parameters of converted phases at various depths more accurately.

For time difference correction with 1D velocity models, we adopt a two-pronged approach: 1D RF inversion or, when applicable, joint inversion with surface dispersion. This method is particularly effective in obtaining an average velocity model for each station. By employing the format required by TauPy, we facilitate the initial estimation of conversion point locations in depth for different Receiver Functions (RFs). This approach not only enhances the accuracy of our depth estimations but also accounts for the complex nature of seismic wave propagation through varying geological structures.

In our comprehensive seismic investigation, we focus on a broad spectrum of discontinuities, extending from the Earth's surface to the mantle

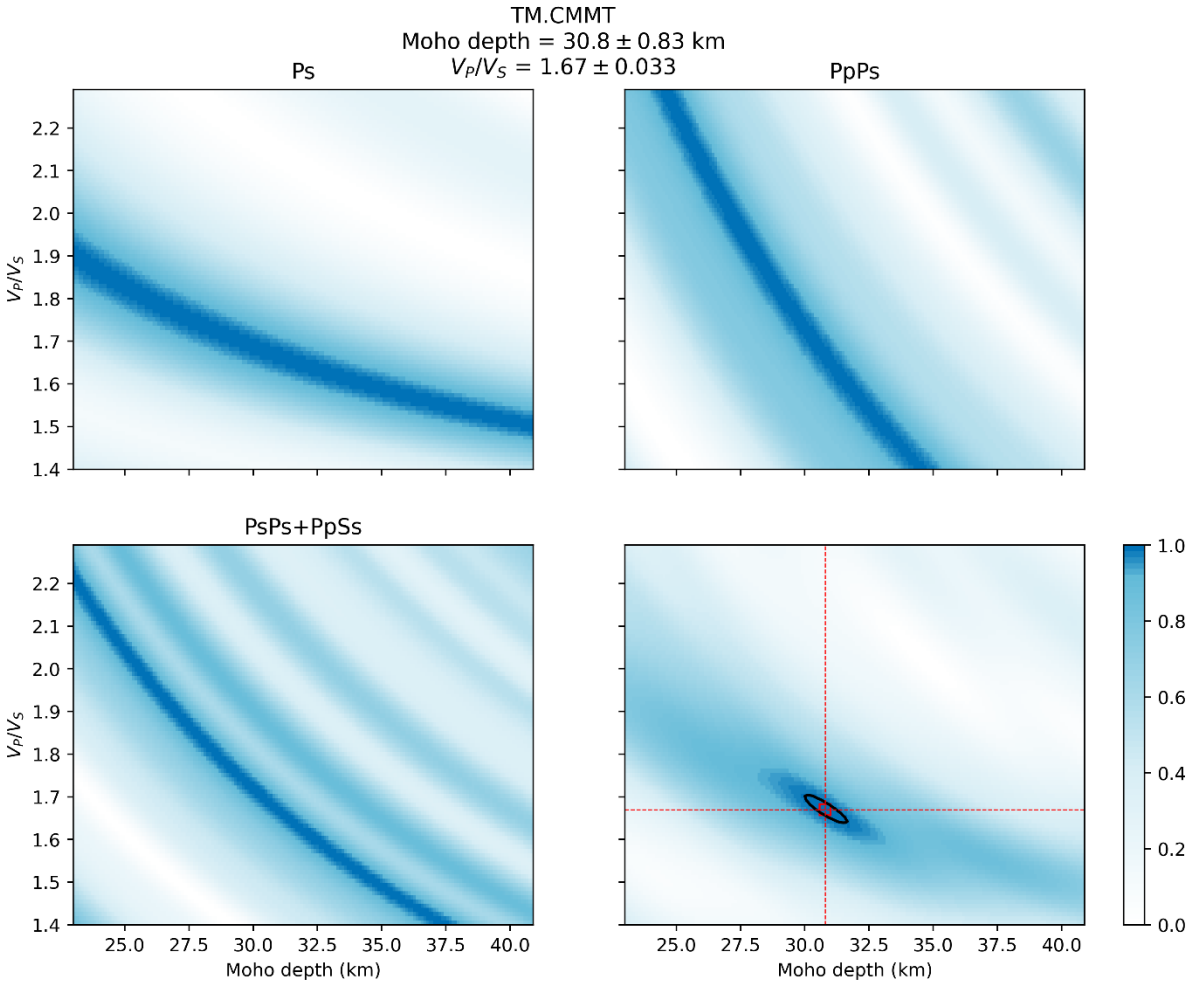

Fig. 3 H-K stacking analysis TM.CMMT. This figure illustrates the H-K stacking analysis at seismic station TM.CMMT, displaying four distinct panels for the phases Ps, PpPs, and the combined PsPs+PpSs. The color scale highlights the amplitude of the stacking function. The analysis determines Moho depth (H) at 30.8 ± 0.83 km and Vp/Vs ratio (k) at 1.67 ± 0.033, within the H range of 23-41 km, as defined by 3D CCP stacking shown in Figures 5 and 7, and k from 1.4 to 2.3. The depth conversion utilizes a crustal Vp of 6.21 km/s (Saetang and Duerrast, 2023).

transition zones at 410 km and 660 km depths. For this, we utilized the GyPSuM 3D velocity model, valued for its ability to accurately represent the extended radius of ray distribution across these significant depths. The analysis methodology begins with the IASP91 model to determine initial conversion point locations, followed by a meticulous interpolation using the GyPSuM 3D model for refinement. Additionally, the Seispy software employ Snell's law under the assumption of a layered model beneath the station, which enables us to approximate the ray parameters as those of the direct primary waves and to calculate the ray incidence angles and conversion point locations for different Receiver Functions (RFs) across each layer using the 3D model. This process is enhanced by interpolating the migrated ray paths within the 3D model, obtaining corrected time differences for converted phases and then interpolating the RF amplitudes with these corrected time differences post station elevation adjustment. This comprehensive approach significantly enhances the precision of time difference calculations across various RFs, a crucial element for accurately delineating converted phases across a wide range of depths.

A pivotal aspect of our research is the application of 3D Common Conversion Point (CCP) Stacking, systematically executed using the Seispy software suite. This sophisticated technique, critical for the accurate extraction of discontinuity depths such as the Conrad and Moho, presents a robust and refined alternative to conventional H-κ stacking methods. It adeptly accounts for complexities such as backazimuth variation and the presence of ambiguous multiples in Receiver Functions (RFs). In our 3D CCP stacking configuration, we have opted for circular bins with a radius of 75 km and a consistent interval of 25 km between bins. This arrangement facilitates comprehensive coverage, with the entire stacking process spanning depths from 0 km to 800 km at

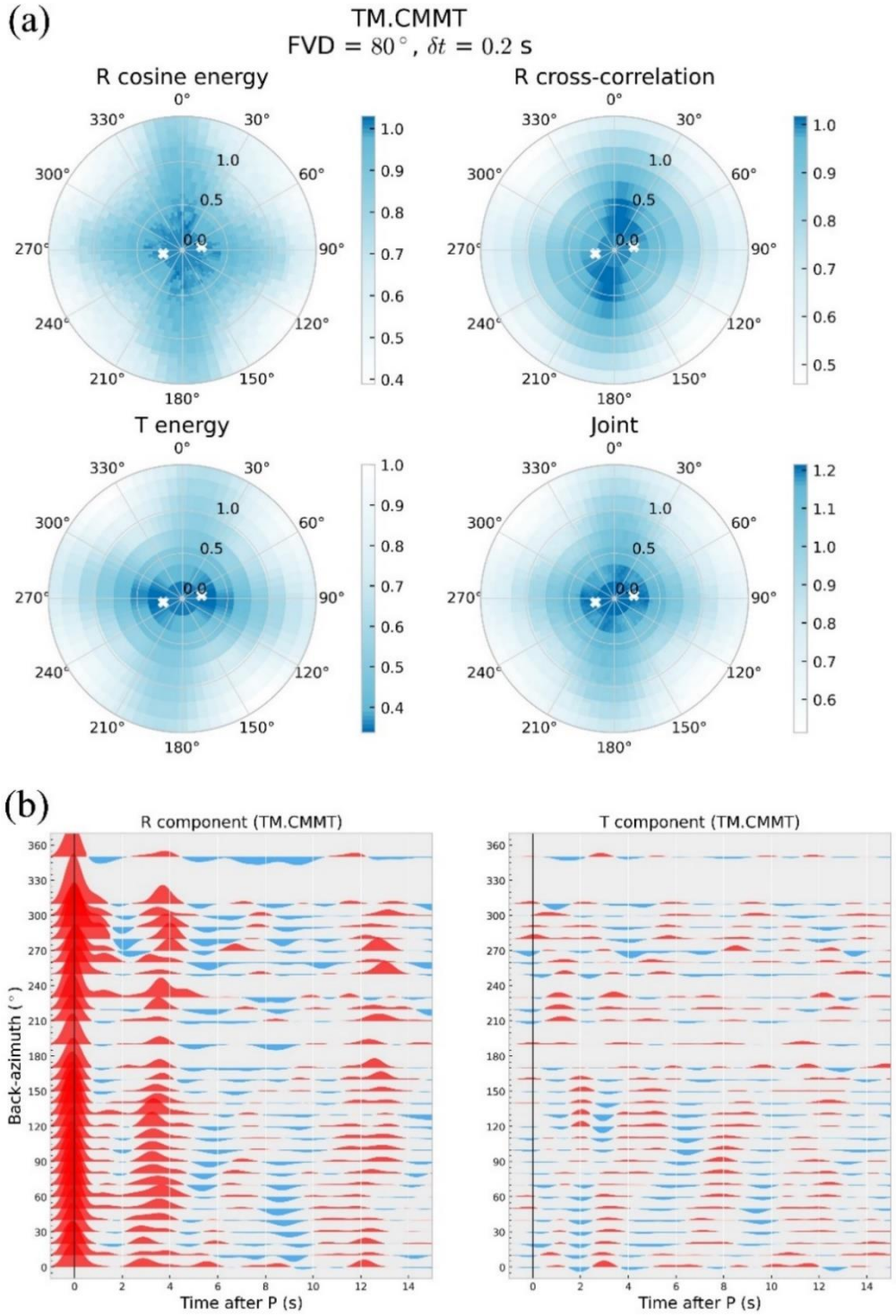

Fig. 4 Anisotropy analysis at station TM.CMMT. (a) Polar plots of radial and transverse component energies correlating with anisotropy, with FVD at 80° and δt of 0.2 s. (b) Waveform variations across back-azimuths aligned with FVD. Results for all stations are compiled in Figure 2 and Table 1.

detailed 1 km intervals. To bolster the reliability of our findings, we have implemented bootstrapping with 1400 boot_samples.

The methodical approach with uniform central angles and depth intervals in circular bins enables a systematic and detailed examination of various deep discontinuities. These include the Conrad and Moho discontinuities, showcased in Figure 5a, as well as the mantle transition zone discontinuities depicted in Figure 5b, beneath Malaysia, Myanmar, and Thailand. A notable feature of the Seispy methodology is the integration of visual depth picking post-3D CCP stacking. This process involves interactively selecting depths for each discontinuity directly from the bins

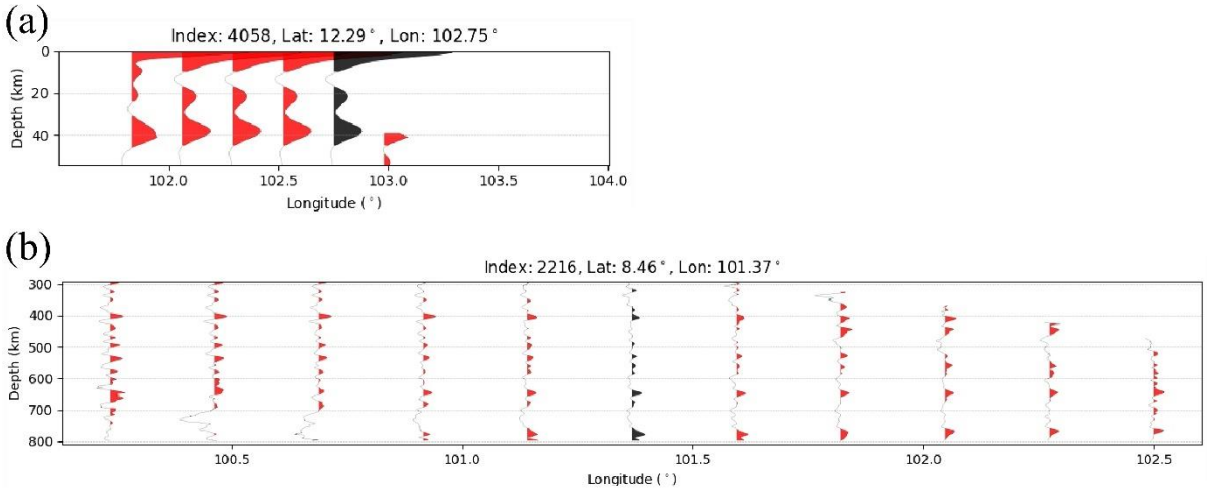

Fig. 5 Seismic discontinuity profiling. (a) depicts the Moho and Conrad discontinuities from 3D CCP stacking, drawn in red at 12.29° latitude and between 102°-103° longitude. (b) illustrates depth variations for the 410 km and 660 km discontinuities at 8.46° latitude, spanning 100.5°-102.5° longitude. The Seispy visual interface is utilized for accurate depth mapping of subsurface features.

using the user interface of Seispy, as demonstrated in Figure 5. This visual approach not only allows for precise depth determination but also provides the flexibility to disregard data from specific bins if deemed unreliable or of poor quality. Through this innovative combination of advanced 3D CCP stacking and user-interactive depth picking, we ensure that our analysis is both thorough and meticulously validated.

3. RESULTS AND DISCUSSIONS

In the ensuing section, we embark on a comprehensive exposition and analysis of the results obtained from our seismic investigation. This segment meticulously delineates the intricate variations in crustal structure and dynamics across Malaysia, Myanmar, and Thailand, revealed through analysis of data from 25 seismic stations. Our discourse focuses on determining the Moho depth (H), the Vp/Vs ratio (k), Conrad depth, the topography of the 410 and 660 km discontinuities, and the multifaceted parameters of crustal anisotropy, revealing the complex seismic characteristics of this geologically diverse region. The juxtaposition of our findings with previous studies unravels both congruencies and disparities, offering a refined understanding of the geophysical characteristics underpinning the area.

3.1. CRUSTAL ANISOTROPY

This study presents new measurements of crustal anisotropy in the Southeast Asian Peninsula using shear-wave splitting analysis of receiver function data. Our results demonstrate a complex pattern of crustal anisotropy that varies across the region, highlighting the intricate interplay of subduction, collision, and crustal deformation processes pivotal in defining the tectonic dynamism of Southeast Asia. The fast polarization directions (ϕ) at stations CRAI, MHIT, and SRDT, for instance, align parallel to significant fault lines—Mae Ing, Mae Hong Son, and Three Pagodas Fault zone, respectively (Fig. 2). This alignment underscores a significant correlation between crustal anisotropy and regional tectonic structures. Additionally, the ϕ of stations CMMT and NGU are parallel to the GPS velocity field, indicating a substantial alignment with the regional kinematic framework. Furthermore, the ϕ at stations NAYO, PRAC, SRIT, and SURA are observed to be closely aligned with the directions of nearby fault lines, further emphasizing the profound influence of local tectonic features on seismic anisotropy. Complementing these observations, the ϕ at stations KUM, SKLT, and TGI are found to be closely aligned with the GPS velocity field, reinforcing the significant correlation between crustal anisotropy and the kinematic patterns dictated by the region's dynamic tectonic processes.

The integrated data from all 25 stations, as represented in Figure 2 and detailed in Table 1, underscore the complexities of these tectonic processes. In Figure 2, the geographical distribution of seismic stations across the Indo-China (ICT), Shan-Thai (STT), and West-Burma (WBT) terranes is precisely mapped, providing a contextual framework for interpreting the comprehensive crustal anisotropy parameters listed in Table 1. These parameters, particularly the ϕ and delay times (δt), serve as key indicators of the seismic fabric and the tectonic stress regime experienced by each terrane. The alignment of ϕ with both fault lines and GPS velocity fields, and its proximity to nearby fault directions at several stations, significantly enriches our understanding of the region's seismic dynamics, offering insights into the intricate relationship between crustal anisotropy, regional tectonics, and the larger geodynamic environment.

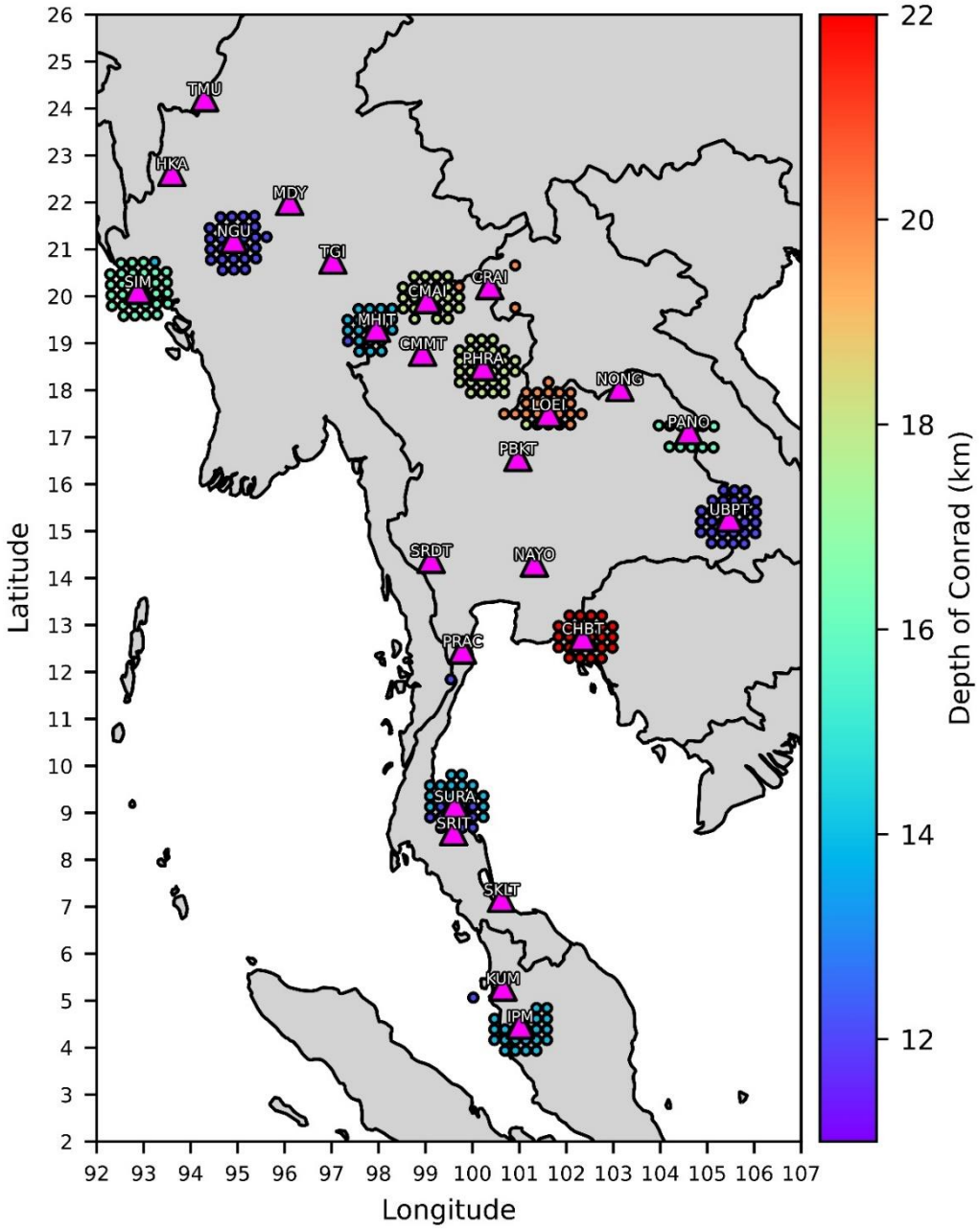

Fig. 6 Depth Variation of the Conrad Discontinuity. Displayed are the Conrad Discontinuity depths across Thailand, Malaysia, and Myanmar, derived from common conversion point stacking. Depths transition from 11 km (violet) to 22 km (red), delineating stratigraphic variation. Seismic stations are marked as magenta triangles, indicating the network's spatial extent.

The interpretation of crustal anisotropy extends beyond these direct alignments, incorporating stations where ϕ directions may not align as clearly with known tectonic features or GPS velocity fields. These stations yield additional insights into the regional tectonic framework, indicating areas influenced by historical tectonic regimes that significantly affect present-day crustal anisotropy. These complexities may reflect mineralogical heterogeneity, preexisting structural features such as foliation or lineation, or reactivated ancient structures. Discrepancies in the alignment of ϕ with GPS velocity fields might signal localized crustal disturbances, such as differential block movements or crustal flexuring, contributing to the seismic wave propagation in the region.

3.2. VARIATIONS OF CONRAD DISCONTINUITY DEPTHS

The Conrad Discontinuity, marking a seismic reflection interface within the Earth's crust, exhibits substantial spatial depth variability across the diverse geological terrains of Malaysia, Myanmar, and Thailand. As illustrated in Figure 6, this discontinuity varies in depth from 11 to 22 km, revealing the

complex stratigraphic and tectonic structure of the lithosphere.

In the West Burma Terrane (WBT), depths recorded around 16 km at station SIM suggest a relatively undisturbed lithospheric structure, indicative of limited recent tectonic activity. In contrast, shallower depths observed at station NGU, around 12 km, imply recent tectonic reshaping, possibly due to orogenic uplift or erosional denudation, in alignment with adjacent fault systems.

Within the Indo-China Terrane (ICT), depths at stations UBPT and PANO, at 11 km and 16 km respectively, point to intricate tectonic interactions. These depth variations are likely caused by extensional forces leading to lithospheric thinning. At the juncture of the Shan-Thai Terrane (STT) and ICT, particularly at stations CHBT and LOEI with depths of 22 km and 20 km, a notable variation in depth is observed, marking a zone of significant lithospheric modification due to continental collision and terrane accretion.

Adjacent to the Khlong Marui Fault zone, depths at stations SRIT and SURA, at 11 km and 15 km respectively, highlight the impact of sedimentation and changes in the crust's thermal regime and mechanical properties. Near the Gulf of Malaysia, station IPM shows a consistent depth of 14 km for the Conrad Discontinuity, in general agreement with the 12 km determination by Latiff and Khalil (2019), suggesting tectonic stability, contrasting with the dynamic geological setting near the Khlong Marui Fault zone.

In Northern Thailand, the Conrad discontinuity depth ranges between 14 and 17 km, reflecting the region's intricate tectonic history shaped by major fault systems and the collisional dynamics of the Western, Central, and Eastern Belts.

3.3. VARIATIONS IN MOHO DEPTH AND VP/VS RATIO

In the realm of earthquake seismology, the determination of Moho depth (H) and the ratio of compressional to shear wave velocities (Vp/Vs) holds paramount significance. The present investigation, employing the H-K stacking method alongside receiver function analysis, spans an array of seismic stations strategically positioned in Thailand, Malaysia, and Myanmar. The resultant data, as detailed in Table 1, indicates a remarkable breadth in Moho depths, ranging from a relatively shallow depth of approximately 26 km at stations SKLT and SIM to a profound depth of 40.5 km at stations TGI and TMU, culminating in an average Moho depth of approximately 32.54 km. Furthermore, the Vp/Vs ratios exhibit significant variability, indicative of the heterogeneous crustal composition across the studied region, spanning from a low of 1.47 at station SIM to a high of 2.20 at station TMU.

The integration of data derived from H-K stacking and CCP stacking, enriched by a critical review of prior studies, offers detailed insights into the lithospheric structure, which is essential for advancing geodynamic modeling and enhancing seismic hazard analysis in this seismically active region. The comprehensive dataset, encapsulated within Table 1 and Figure 7, provides a broad perspective on the subsurface architecture, significantly enriching our understanding of Southeast Asia's geodynamics. This synthesis of quantitative and visual data serves as a crucial foundation for seismic risk assessment, emphasizing the importance of Moho depth variability and its implications for understanding seismic activity and the complexity of crustal dynamics across the area.

3.3.1. COMPARATIVE ANALYSIS OF H-K STACKING OUTCOMES WITH PRIOR STUDIES AND CCP STACKING RESULTS

The Moho depth at station TGI is determined to be 40.50±1.02 km with a corresponding Vp/Vs ratio of 1.690±0.027 through H-K stacking methodology. These determinations are consistent with the common conversion point stacking outputs, which manifest a depth proximate to 38 km, depicted in orange, around station TGI in Figure 7. This depiction contradicts the depth of 33 km and Vp/Vs ratio of 1.84 previously delineated by Nwe et al. (2022), thereby highlighting the profound impact that disparate methodological applications in H-K stacking may have upon seismic analytical outcomes.

The Moho depth estimations at station CHBT, as calculated in the present study, stand at 38.50±0.61 km with a corresponding Vp/Vs ratio of 1.730±0.056. These results are substantiated by the common conversion point stacking method, as delineated in Figure 7, where a depth of approximately 38 km is demarcated in red near the station, a measure notably deeper than the 28.96 ± 0.90 km depth with a Vp/Vs ratio of 1.760 ± 0.019 as delineated by Noisagool et al. (2014). Such disparities may originate from the discrete methodological approaches implemented in H-K stacking, where variable assumptions of P-wave velocities, selection of receiver functions, and differing treatments of seismic noise can significantly influence the analytical results.

Additionally, the Moho depths at station TMU are meticulously measured through H-K stacking as 40.50±0.06 km with a Vp/Vs ratio of 2.203±0.002. While the common conversion point stacking technique, as depicted in Figure 7, indicates a depth slightly shallower at approximately 35 km, it is still significantly shallower than the 50.5 km depth with a Vp/Vs ratio of 1.99 reported by Nwe et al. (2022). This variance in depth estimations and Vp/Vs ratios, especially in the vicinity of station TMU, suggests complex lithospheric dynamics that may not be fully captured by a single methodological approach.

For station CMAI, located in the northern Thailand, the elucidation of Moho depth via the H-K stacking approach in the present study reveals a depth of 30.50±1.06 km coupled with a Vp/Vs ratio of 1.760±0.042. This depth is in close accordance with

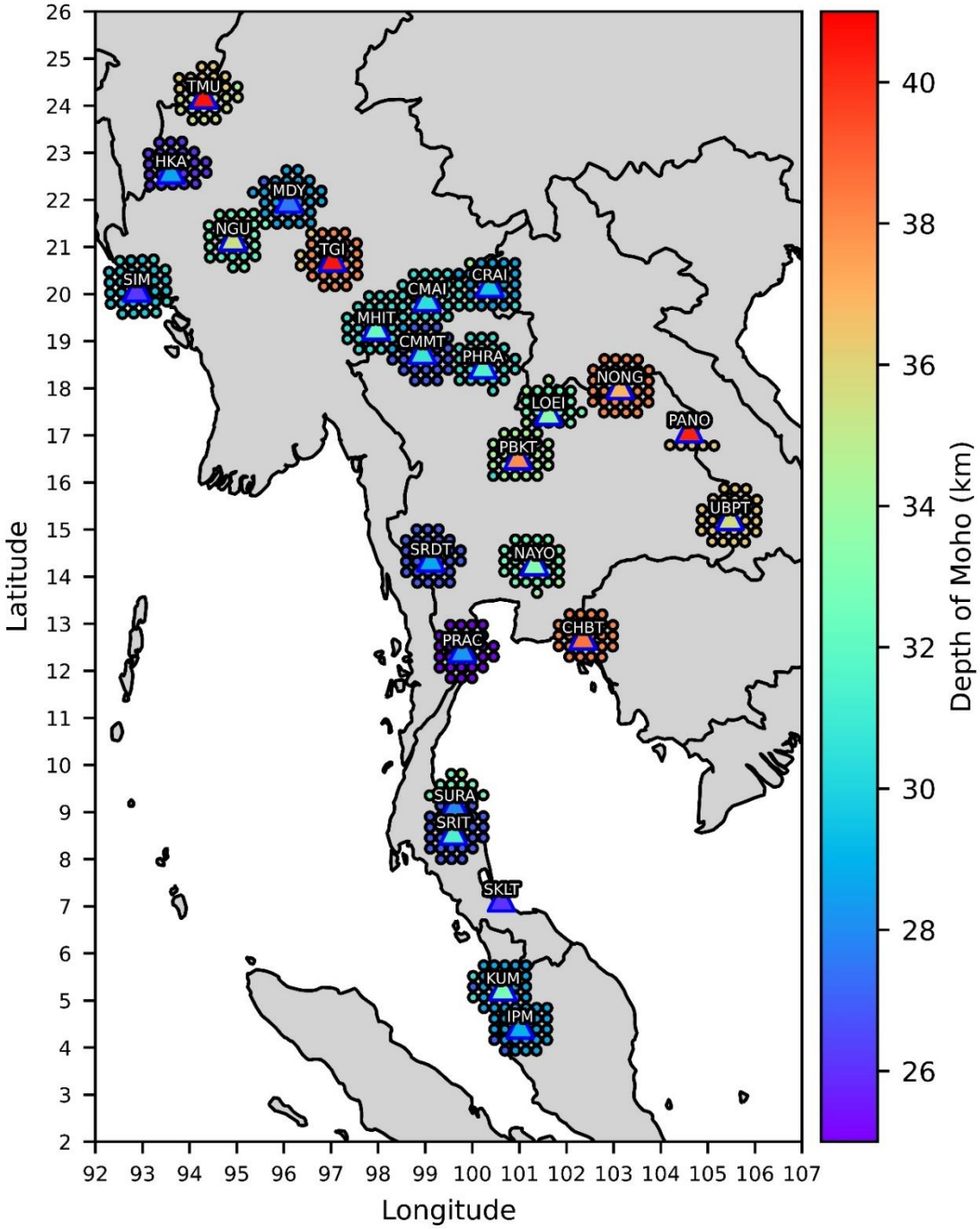

Fig. 7 Moho depth distribution in Thailand, Malaysia, and Myanmar. Displayed are Moho depths derived from H-K stacking (triangles) and common conversion point stacking (dots), ranging from 25 km (violet) to 41 km (red), illustrating the tectonic complexity of the region.

findings by Noisagool et al. (2014), who published a Moho depth of 32.20±0.44 km and a Vp/Vs ratio of 1.740±0.012, and is further validated by a CCP stacking result indicating a Moho depth of 30 km. This congruence across methodological spectra highlights the intrinsic variability characteristic of seismic investigations, affirming the robustness and consistency of geophysical analyses.

Station IPM, strategically located at the peninsular region of Malaysia, manifests a Moho depth of 29.00±0.48 km with a Vp/Vs ratio of 1.770±0.026 ascertained through this investigation's H-K stacking technique. This result aligns with the Moho depth range of 24-32 km and a Vp/Vs ratio of 1.79 proposed by Latiff and Khalil (2019), mirroring the region's geological diversity, and concurs with the CCP stacking methodology indicating a similar Moho depth of 29 km. Such alignment corroborates the precision of seismic methodologies in discerning the subsurface structure.

The analytical scrutiny at station NAYO discloses a Moho depth of 33.20±0.76 km and a Vp/Vs

ratio of 1.750±0.030, revealing the complex geological structure of Thailand. This depth deviates from the 35.18±1.70 km depth by Noisagool et al. (2014), underscoring the impact of localized geological formations on seismic wave propagation. The noted discrepancy between H-K stacking outcomes and antecedent studies accentuates the dynamic geological framework of the region, with CCP stacking results paralleling this study's findings at 33 km, thereby reinforcing the validity of seismic interpretations.

In the case of station NONG, the investigation delineates a Moho depth of 36.90±0.94 km with a Vp/Vs ratio of 1.750±0.029, indicative of a comparatively thicker crust within the examined locale. This finding corroborates the prior estimate of 39.28±0.42 km by Noisagool et al. (2014), reflecting the geological intricacies of the area. The CCP stacking outcome, indicating a Moho depth of 38 km, aligns closely with these observations, highlighting the significance of employing a multifaceted approach in seismic analysis to unravel the complexities of crustal architecture.

Station PBKT indicates a Moho depth of 37.90±0.81 km with a Vp/Vs ratio of 1.680±0.028. This measurement is slightly beneath the depth of 40.03±0.24 km reported by Noisagool et al. (2014), demonstrating the heterogeneity of the crust beneath Thailand. The comparative analysis with CCP stacking outcomes, which suggest a shallower depth of 34 km, enriches the understanding of subsurface discontinuities, demonstrating the imperative of integrating diverse seismic methodologies for a comprehensive geological model.

Station CRAI provides an illustrative example, wherein the Moho depth, ascertained through H-K stacking, is discerned to be 29.70±0.86 km with a Vp/Vs ratio of 1.740±0.034. The Common Conversion Point (CCP) stacking method corroborates this finding, estimating the Moho depth at 29 km. Notably, this station's H-K stacking-derived Moho depth has not been previously reported in the literature, thereby contributing novel insights into the seismic structure beneath the region.

In the case of Station HKA, located within the West Burma Terrane (WBT), a Moho depth of 28.70±0.01 km and a Vp/Vs ratio of 1.66±0.001 are determined through H-K stacking. This outcome markedly contrasts with the findings of Nwe et al. (2022), which indicate a substantially deeper Moho at 49.4 km. Such a discrepancy could potentially be attributed to localised geological variations or to the inherent sensitivity of the H-K stacking method to specific seismic waveform characteristics. In accordance with this study, the CCP stacking analysis suggests a Moho depth around 25 km, underscoring the variability inherent in seismic data interpretation.

Station KUM, reflecting the geologic heterogeneity of the Malay Peninsula, reveals a Moho depth of 32.80±0.59 km with a Vp/Vs ratio of 1.710±0.027. This depth aligns approximately with the 30 km Moho depth and 1.73 Vp/Vs ratio reported by Latiff and Khalil (2019), further validated by a CCP stacking-derived depth of 28 km. This consistency across diverse methodologies underscores the reliability of seismic analysis in delineating crustal structures.

Station LOEI, situated amidst the complex geological landscape of northeastern Thailand, yields a Moho depth of 33.40±1.34 km and a Vp/Vs ratio of 1.740±0.048. This result resonates with the Moho depth of 34.92±1.23 km and Vp/Vs ratio of 1.740±0.013 as reported by Noisagool et al. (2014). Furthermore, the CCP stacking method estimates a Moho depth of 32 km, affirming the coherence between different seismic analysis techniques and highlighting the dynamic geological evolution of the region.

Station MDY, positioned in central Myanmar, exhibits a Moho depth of 27.50±1.31 km and a Vp/Vs ratio of 1.77±0.060. This contrasts with the Moho depth of 35.5 km and Vp/Vs ratio of 1.60 reported by Nwe et al. (2022), and differs from a CCP stacking-derived depth of 27 km, indicating the complex interplay of geological processes influencing seismic wave propagation in this region.

Station UBPT, elucidating the crustal features of northeastern Thailand, records a Moho depth of 35.60±2.69 km and a Vp/Vs ratio of 1.750±0.066, consistent with the CCP stacking method which indicates a Moho depth of 35 km. This finding aligns closely with the Moho depth of 33.67±2.76 km reported by Noisagool et al. (2014), showcasing the robustness of integrated seismic methodologies in capturing the intricate structure of Earth's lithosphere.

The application of the H-K stacking method at station PRAC reveals a Moho depth of 28.20 ± 0.61 km with a Vp/Vs ratio of 1.690 ± 0.026. This finding is in approximate agreement with the results of Noisagool et al. (2014), who documented a Moho depth of 30.04 ± 0.45 km and a Vp/Vs ratio of 1.660 ± 0.011. However, the Common Conversion Point (CCP) stacking results, indicating a shallower Moho depth of 25 km, introduce a notable disparity. This discrepancy may allude to the geological complexity of the region, implying potential variations in crustal composition or tectonic activity that warrant further investigation.

At station SIM, the determined Moho depth is 26.20 ± 0.64 km with a Vp/Vs ratio of 1.470 ± 0.032. This outcome is congruent with the findings of Nwe et al. (2022), who reported a similar Moho depth of 26.0 km and a Vp/Vs ratio of 1.50. The CCP stacking results, however, suggest a marginally deeper depth of 29 km, thereby introducing a subtle yet significant variation that might reflect underlying heterogeneities in the subsurface structure.

Station SURA, located in the Gulf of Thailand, records a Moho depth of 27.90 ± 1.02 km and a Vp/Vs ratio of 1.810 ± 0.064. These findings closely align

with those reported by Latiff and Khalil (2019), who observed a Moho depth of 28 km and a Vp/Vs ratio of 1.82. Nevertheless, the CCP stacking results indicate a slightly deeper depth of 33 km, potentially suggesting the presence of more complex subsurface structures or variations in seismic wave velocities within the region.

The H-K stacking method applied at station CMMT has determined a Moho depth of 30.80 ± 0.80 km and a Vp/Vs ratio of 1.670 ± 0.032. This finding aligns closely with previous research conducted by Noisagool et al. (2014), who reported a Moho depth of 32.31 ± 0.33 km and a Vp/Vs ratio of 1.670 ± 0.031. The Common Conversion Point (CCP) stacking results, however, indicate a shallower Moho depth of approximately 26 km. This discrepancy between the H-K stacking and CCP stacking methodologies may suggest an intricate geological fabric beneath the station, potentially indicating variations in crustal composition or tectonic influences that affect seismic wave propagation.

For station MHIT, the deployment of the H-K stacking method has discerned a Moho depth of 32.20 ± 0.78 km and a Vp/Vs ratio of 1.710 ± 0.033. This determination exhibits a notable correspondence, albeit with slight variance, to the results obtained by Noisagool et al. (2014), who delineated a Moho depth of 34.59 ± 0.24 km and a Vp/Vs ratio of 1.67 ± 0.009. The observed variation in Moho depth estimations between these studies is indicative of the underlying complex geological structures at this station. Furthermore, the Common Conversion Point (CCP) stacking results suggest a Moho depth of approximately 30 km, which, while slightly shallower than the findings of Noisagool et al. (2014), is congruent with the results derived from our H-K stacking analysis.

For station NGU, the application of the H-K stacking method indicates a Moho depth of 35.40 ± 0.86 km and a Vp/Vs ratio of 1.890 ± 0.024. This finding aligns with the results presented by Nwe et al. (2022), who reported a comparable Moho depth of 34.5 km and a Vp/Vs ratio of 1.94. However, the Common Conversion Point (CCP) stacking analysis provides a somewhat contrasting perspective, suggesting a marginally shallower Moho depth of approximately 32 km.

At station PANO, the H-K stacking methodology determined a Moho discontinuity at a depth of 40.30 ± 1.70 km and a Vp/Vs ratio of 1.680 ± 0.063. The lack of previous research on station PANO limits the ability for direct comparison with the existing literature. Crucially, analysis through Common Conversion Point (CCP) stacking offers additional insights, suggesting a Moho depth of approximately 37 km. This CCP-derived depth, slightly shallower than that obtained via H-K stacking, underscores the heterogeneity and complexity of the crustal features beneath PANO.

Utilising the H-K stacking methodology at station SKLT, the investigation has ascertained a Moho discontinuity at a depth of 26.10 ± 0.67 km, accompanied by a Vp/Vs ratio of 1.670 ± 0.031. These findings exhibit coherence with the outcomes presented by Noisagool et al. (2014), wherein the Moho depth was characterised as 27.44 ± 0.25 km with a Vp/Vs ratio of 1.670 ± 0.009. It is noteworthy, however, that the Common Conversion Point (CCP) stacking technique did not yield results for station SKLT. The absence of CCP stacking data may stem from various factors, including limitations in data quality, coverage, or the specific geophysical characteristics of the region that preclude effective application of this method for the station in question.

For station SRDT, the H-K stacking method delineated a Moho discontinuity at a depth of 28.80 ± 0.68 km with an accompanying Vp/Vs ratio of 1.690 ± 0.027. This analysis contributes critically to the delineation of crustal architecture beneath the station. The results are in consonance with those reported by Noisagool et al. (2014), who characterized the Moho depth at approximately 29.74 ± 0.53 km with a Vp/Vs ratio of 1.680 ± 0.016. Complementary to this, the Common Conversion Point (CCP) stacking analysis suggests a Moho depth proximal to 26 km, which, albeit slightly shallower, is consistent with the general geologic characteristics of the region as observed in prior studies.

At station SRIT, located within the complex geological milieu of the Gulf of Thailand, the H-K stacking methodology showed a Moho depth of 31.40 ± 0.55 km and a Vp/Vs ratio of 1.650 ± 0.025. These determinations closely align with the findings by Latiff and Khalil (2019), who documented a Moho depth at approximately 28 km with a Vp/Vs ratio of 1.77. The CCP stacking analysis, indicating a Moho depth near 26 km, underscores the intricate geological dynamics underpinning this locale. The observed disparity in Moho depths between the H-K and CCP stacking analyses could reflect the influence of unaccounted structural heterogeneities or the dynamics associated with sedimentary basin evolution.

3.3.2. GEOLOGICAL INTERPRETATIONS AND IMPLICATIONS OF SEISMIC DATA VARIABILITY

The detailed seismic investigation across Thailand, Malaysia, and Myanmar, leveraging both H-K stacking and CCP stacking methodologies, has revealed significant variations in Moho depths and Vp/Vs ratios, which, when aligned with the geological terranes of each station, indicate the complex tectonic narratives of the region. This synthesis integrates latitudinal and longitudinal data to provide a geologically informed interpretation of seismic observations, shedding light on the interplay between crustal properties and tectonic evolution.

In the intricate geodynamic landscape of the West Burma Terrane, seismic evaluations at stations SIM, HKA, NGU, TMU, and MDY indicate a diverse crustal fabric, as evidenced by the comprehensive seismic data gathered through both H-K stacking and

Common Conversion Point (CCP) stacking techniques. Results indicate variable crustal thicknesses, with station TMU (H-K: 40.50 km, CCP: 35 km, Vp/Vs: 2.203) exhibiting the greatest depth. This pronounced crustal thickening is likely related to subduction processes beneath the Sunda megathrust (Biswas and Gangumalla, 2021; Hurukawa et al., 2012). This observation is complemented by station NGU (H-K: 35.40 km, CCP: 32 km, Vp/Vs: 1.890), which also suggests a significant crustal thickening. In contrast, stations HKA (H-K: 28.70 km, CCP: 25 km, Vp/Vs: 1.66) and SIM (H-K: 26.20 km, CCP: 29 km, Vp/Vs: 1.47) reveal shallower Moho depths.

The analysis of Common Conversion Point (CCP) stacking outcomes indicates a pronounced variation in crustal thickness traversing the Sagaing Fault, thereby articulating a stark contrast in the lithospheric architecture across this tectonic boundary. Specifically, observations at station MDY, which is situated along the western margin of the Sagaing Fault and exhibits a Moho depth of 27.50 km (with CCP-derived depth at 27 km and Vp/Vs ratio at 1.77), denote a relatively attenuated crustal section in comparison to the findings at station TGI, positioned on the fault's eastern flank. At this latter station, the CCP methodology delineates a Moho depth of 38 km (with H-K stacking revealing 40.50 km and Vp/Vs ratio at 1.69), significantly deeper than that recorded at MDY. The increase to approximately 38 km depth, determined from CCP stacking, indicates significant crustal thickening, emphasizing the role of the Sagaing Fault in influencing subsurface structural variations.

In the northern Thailand, within the Shan-Thai Terrane, observations from seismic stations, namely CMAI, CRAI, MHIT, CMMT, and PHRA, indicate the terrane's geological intricacies through the variability in Moho depths and Vp/Vs ratios. The H-K stacking analyses divulge Moho depths extending from approximately 29.70 km at CRAI to 32.20 km at MHIT, with the corresponding Vp/Vs ratios ranging from 1.670 at CMMT to 1.760 at CMAI. Complementary results, derived from Common Conversion Point (CCP) stacking, further refine our comprehension by delineating Moho depths that are broadly congruent with the findings from H-K stacking, ranging from 26 km at CMMT to 30 km at CMAI, MHIT, and PHRA. These determinations underscore the significant variations in crustal thickness across this terrane.

Within the complex geological framework of the Shan-Thai Terrane, seismic analyses at stations LOEI, PBKT, NAYO, and CHBT provide critical insights into the Moho depth variations, revealing a ronounced trend of increasing depth closer to the boundary with the Indo-China Terrane. Station LOEI, showing a Moho depth of 33.40 km and a Vp/Vs ratio of 1.740 via H-K stacking, corroborated by a CCP depth of 32 km. Station PBKT, with a Moho depth of 37.90 km and a Vp/Vs ratio of 1.680 (H-K stacking), and a CCP determined depth of 34 km. Notably, station NAYO, strategically situated near the terrane boundary, reveals a Moho depth of 33.20 km and a Vp/Vs ratio of 1.750, with CCP stacking affirming a depth of 33 km, further emphasising the trend of increasing Moho depth towards the terrane interface. Station CHBT, at the boundary, with a Moho depth of 38.50 km and a Vp/Vs ratio of 1.730 (H-K stacking), and a CCP depth of 38 km, underscores the remarkable crustal depths encountered at the margin of the Shan-Thai and Indo-China terranes. The substantial depths observed at CHBT, along with the gradational increase highlighted by LOEI, PBKT, and NAYO, accentuate the significant geological impact of the neighbouring Indo-China Terrane. This gradational deepening of the Moho is indicative of the differential geodynamic processes operative within the terrane (Knapmeyer-Endrun et al., 2014).

These findings, as shown for Moho depths (Fig. 7) and Conrad discontinuity depths (Fig. 6) across the Shan-Thai and adjacent terranes, provide a comprehensive overview of the lithospheric structure. The consistency across H-K and CCP methodologies not only affirms the robustness of seismic analysis but also highlights the intricacies of crustal dynamics influenced by the neighboring Indo-China Terrane. This complex crustal interaction, underscored by a gradational increase in depth towards the terrane boundary, is emblematic of the region's dynamic geodynamics. It suggests a complex interplay of tectonic forces that have been instrumental in sculpting the seismotectonic fabric of the area, revealing the significant geological impact and the profound tectonic interactions that characterize the transition from the Shan-Thai to the Indo-China Terrane.

Within the Indo-China Terrane, seismic studies at stations NONG, PANO, and UBPT have been pivotal in delineating the terrane's seismotectonic characteristics, revealing pronounced crustal thickening when contrasted with the Shan-Thai Terrane. At NONG, the determined Moho depth of 36.90 km and Vp/Vs ratio of 1.750, validated by CCP findings of 38 km, illustrates a significantly thicker crust than that observed within the Shan-Thai Terrane, suggesting active tectonic dynamics possibly influenced by lithospheric extension and mantle processes. Similarly, at PANO, a Moho depth of 40.30 km and Vp/Vs ratio of 1.680, with CCP corroborating a depth of around 37 km, highlights a robust crustal thickening reflective of the terrane's intricate collisional history and ongoing crustal modifications. UBPT, located at the terrane's eastern frontier, evidences a Moho depth of 35.60 km and a Vp/Vs ratio of 1.750, with CCP depth affirmation at 35 km, further attesting to the significant crustal thickening, indicative of the complex tectonic narrative. These observations collectively emphasize the notable crustal thickening within the Indo-China Terrane, markedly contrasting with the Shan-Thai Terrane's Moho depth profiles, thus underscoring the distinct geological and geodynamic vigor of the Indo-China Terrane.

In the geophysically intricate domain of Southern Thailand, particularly in the vicinity of the Khlong Marui Fault Zone and adjacent to the Gulf of Thailand, seismic stations SURA and SRIT (Fig. 2 and Fig. 7) provide pivotal insights into the crust dynamics through a detailed analysis of Moho depth and Vp/Vs ratios, utilizing both H-K stacking and Common Conversion Point (CCP) stacking methodologies. SURA's analysis delineates a Moho depth of 27.90 km with a Vp/Vs ratio of 1.810, nuanced by a CCP depth of 33 km. Similarly, SRIT reports a Moho depth of 31.40 km and a Vp/Vs ratio of 1.650, with CCP stacking presenting a depth of 26 km, underscoring a substantial crustal thickness reflective of the region's active tectonic regime yet indicating shallower crustal thickness compared to the more profound depths observed in the Indo-China Terrane. These critical assessments from SURA and SRIT underscore the Khlong Marui Fault Zone's and the Gulf of Thailand's significant roles in modulating the seismic landscape, highlighting areas of shallower crustal thickness that contrast markedly with the greater depths charted within the Indo-China Terrane.

In the geodynamic landscape of the Gulf of Malaysia, the seismic stations KUM and IPM offer an in-depth perspective into the lithospheric nuances of this maritime region, through the adept use of H-K stacking and Common Conversion Point (CCP) stacking analyses. Station KUM, registering a Moho depth of 32.80 km and a Vp/Vs ratio of 1.710 (H-K stacking) and a CCP depth of 28 km, reveals a crustal composition that, while substantial, presents a marked contrast to the deeper profiles identified within the Indo-China Terrane. Similarly, IPM, with its Moho depth of 29.00 km and a Vp/Vs ratio of 1.770 (H-K stacking), corroborated by a CCP depth of 29 km, further evidences this trend of relatively shallower crustal thickness when juxtaposed against the pronounced depths charted across the Indo-China Terrane. Such comparative analysis underscores a discernible difference in crustal dynamics between the Gulf of Malaysia and the Indo-China Terrane, highlighting a geophysical demarcation that might be attributable to varied tectonic histories and current geodynamic processes.

3.4. DEPTH VARIATIONS OF THE 410 KM SEISMIC DISCONTINUITY

The 410 km discontinuity delineates a pivotal boundary within the Earth's mantle, representing the phase transition from olivine to wadsleyite, as determined by Katsura et al. (2010). This boundary is instrumental in understanding the intricate dynamics and compositional stratification of the mantle. The depth distribution of the 410 km seismic discontinuity across Southeast Asia, as depicted in Figure 8, exhibits a remarkable range of depths, from approximately 388 km (represented in violet, denoting shallower regions) to around 436 km (illustrated in red, indicating deeper segments). Such variability in depth underscores the spatial heterogeneity of the mantle transition zone, reflecting a complex interplay between tectonic activity and mantle dynamics.

The analysis of depth variations reveals a pronounced aggregation of shallower depths within the Gulf of Malaysia. This observation, combined with the geological and tectonic features delineated in Figure 2, suggests that the mantle beneath this region has been subject to thermal modification, likely attributable to tectonic thinning and extensional processes. This inference is supported by the spatial correlation of these shallower depths with significant extensional features, such as the Khlong Marui Fault zone, implying that these geological processes have left a discernible thermal imprint on the mantle structure, observable in the diminished depths of the discontinuity.

In contrast, the West Burma Terrane is characterized by a spectrum of depths from intermediate to deeper values, represented by hues ranging from orange to red. This depth variation can be attributed to the complex subduction dynamics where the Indian Plate subducts beneath the Eurasian Plate. The detailed GPS velocity fields and the geological intricacies of collision and subduction zones within this terrane, as illustrated in Figure 2, likely exert a significant influence on the mantle configuration beneath, contributing to the observed depth variations. The intermediate depth range, encapsulated by hues of intermediate intensity, may signify the presence of an extensional tectonic regime within the basin. This regime hints at an upwelling of thermally enriched mantle material, a hypothesis further substantiated by the distribution of GPS velocity vectors and the manifestation of crustal anisotropy. Such geological indicators suggest ongoing tectonic deformation, potentially facilitating mantle upwelling, thereby impacting the thermal state of both the lithosphere and asthenosphere.

The depth distribution of the 410 km discontinuity, therefore, offers invaluable insights into the thermal and compositional dynamics of the mantle beneath Southeast Asia. It highlights the significance of integrating seismic data with tectonic and geological frameworks to indicate the complex processes governing mantle dynamics and structure.

3.5. DYNAMICS OF THE 660 KM DISCONTINUITY

The dynamics of the 660 km discontinuity within the mantle transition zone beneath the geologically complex terrains of Malaysia, Myanmar, and Thailand are identified through a detailed color-coded visual representation in Figure 9. This visualization employs a gradient from violet (representing the shallowest depths, approximately 622 km) to red (denoting the deepest extents, around 690 km), effectively mapping the spatial variability of this fundamental boundary. Such a depiction is instrumental in understanding the nuanced interplay between thermal, compositional, and dynamic processes within the mantle.

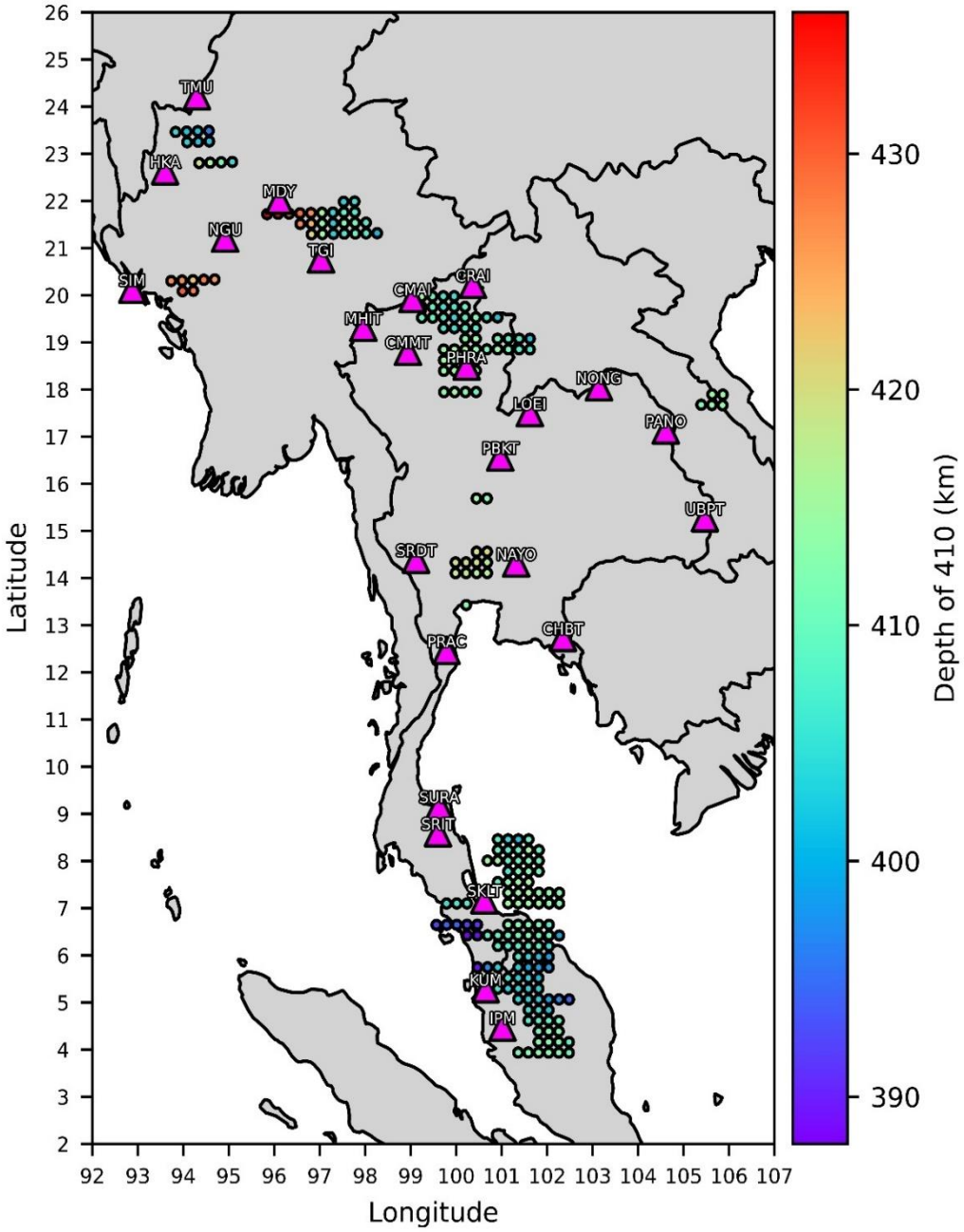

Fig. 8 Spatial Distribution of the 410 km Seismic Discontinuity Depth Across Southeast Asia. This illustration delineates the heterogeneity in the depth of the 410 km seismic discontinuity beneath the Southeast Asian region, employing a spectral gradient to represent depth variations. The depths are quantitatively mapped, spanning from a minimum of 388 km to a maximum of 436 km, thereby providing a comprehensive visualisation of the mantle transition zone's topography within this geologically dynamic area.

Upon meticulous examination of the depth data, a discernible spatial correlation emerges, particularly between the shallower depths, illustrated in violet and blue hues, and the Gulf of Malaysia and the Gulf of Thailand. This correlation may signify regions where the asthenosphere is experiencing upwelling, possibly as a consequence of historical tectonic phenomena, including the South China Sea's opening (Xue et al., 2013; Yu et al., 2018). This upwelling is indicative of active mantle processes that could influence surface geology and seismicity.

4. CONCLUSIONS

The comprehensive seismic analysis across the West Burma Terrane, Shan-Thai Terrane, Indo-China Terrane, and the vicinities of the Gulf of Thailand and Gulf of Malaysia, utilized advanced H-K stacking and Common Conversion Point (CCP) stacking methodologies. This analysis has revealed intricate patterns of crustal anisotropy, Conrad discontinuity variations, and depth fluctuations at the 410 km and 660 km discontinuities. These observations provide detailed insight into the complex geodynamic

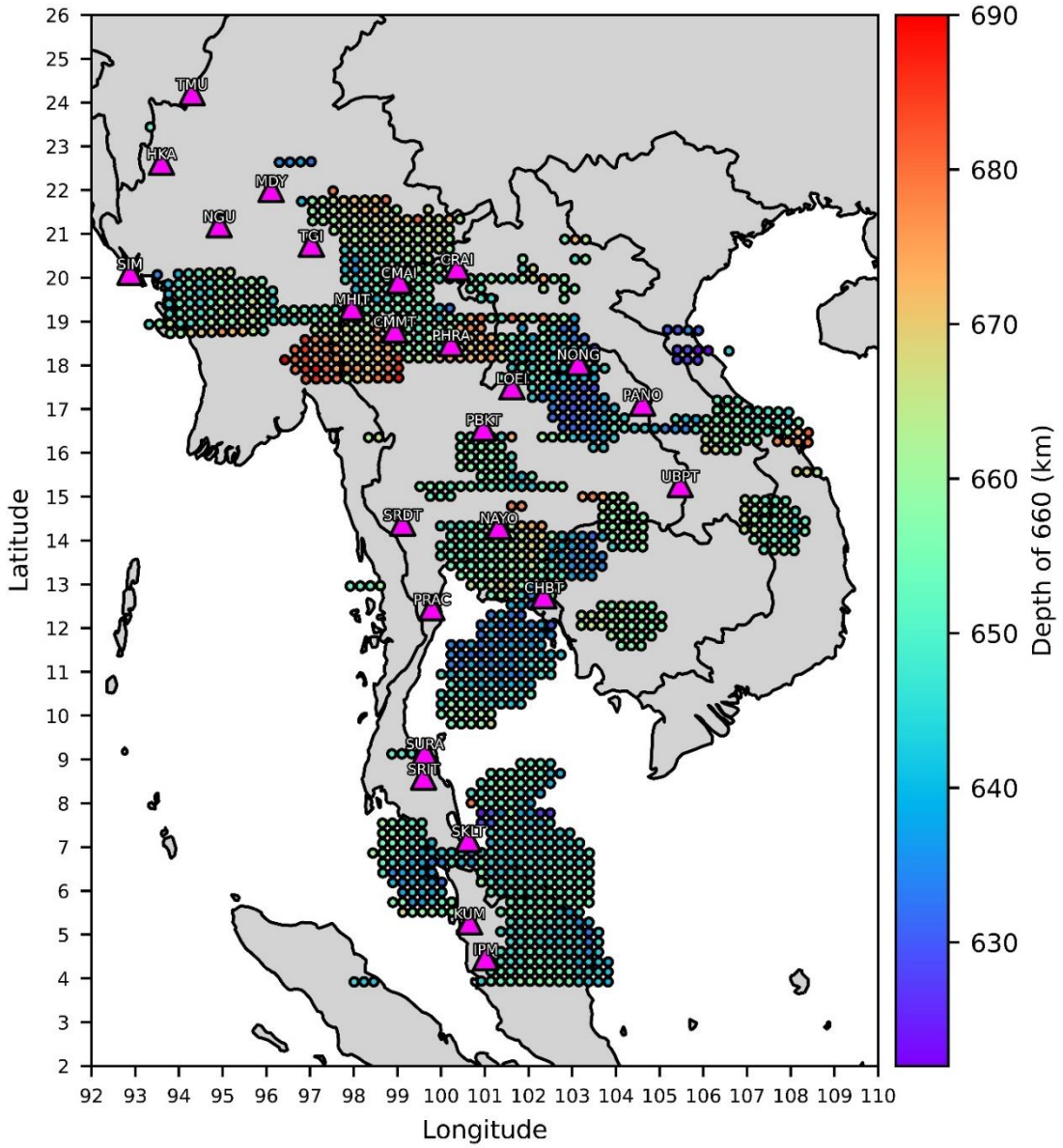

Fig. 9 Detailed mapping of the 660 km discontinuity depth in Southeast Asia. This mapping determines the spatial heterogeneity in the depths of this discontinuity, which range from a minimum of approximately 622 km to a maximum of nearly 690 km.

processes shaping the subsurface structure of Southeast Asia. In the West Burma Terrane, significant crustal thickening is observed, potentially indicative of subduction processes beneath the Sunda megathrust, with variations in the 410 and 660 km discontinuity depths suggesting complex subduction dynamics and mantle upwelling. The Shan-Thai Terrane exhibits a gradational increase in Moho depth towards its boundary with the Indo-China Terrane, reflecting tectonic evolution influenced by collisional dynamics, crustal thickening, and variations in the Conrad discontinuity that underscore the terrane's intricate geological and tectonic history. The Indo-China Terrane demonstrates notable crustal thickening compared with the Shan-Thai Terrane, with depth distribution of the 410 km discontinuity highlighting robust crustal thickening reflective of its intricate collisional history and ongoing crustal modifications. Observations in the Gulf regions suggest shallower crustal thickness and potential mantle upwelling, emphasizing the significant role of crustal anisotropy, Conrad discontinuity depth variations, and deep mantle processes in understanding the interplay between tectonic activity, mantle dynamics, and seismic behavior, providing essential insights for seismic risk assessment and geodynamic modeling in Southeast Asia.

ACKNOWLEDGMENTS

The authors acknowledge the Thai Meteorological Department and the Incorporated Research Institutions for Seismology for providing seismic data, and thank Mijian Xu for the Seispy software utilized in this analysis.

REFERENCES

Beyreuther, M., Barsch, R., Krischer, L., Megies, T., Behr, Y. and Wassermann, J.: 2010, Obspy: A python toolbox for seismology. Seismol. Res. Lett., 81, 3, 530–533. DOI: 10.1785/gssrl.81.3.530

Biswas, A. and Gangumalla, S.R.: 2021, Modelling the Moho depth and Flexure parameters across the Indo-Burma subduction zone. EGU Gen. Assem. 2021, online, 19–30 Apr. 2021, EGU21-6208. DOI: 10.5194/egusphere-egu21-6208

Charusiri, P., Clark, A.H., Farrar, E., Archibald, D. and Charusiri. B.: 1993, Granite belts in Thailand: Evidence from the 40Ar/39Ar geochronological and geological syntheses. J. Southeast Asian Earth Sci., 8, 1, 127–136. DOI: 10.1016/0743-9547(93)90014-G

Cobbing, E.J.: 2011, Granitic rocks. In: Ridd, M.F., Barber, A.J. and Crow, M.J. (Eds.), The Geology of Thailand. Geological Society of London.

Crotwell, H.P., Owens, T.J. and Ritsema, J.: 1999, The taup toolkit: Flexible seismic travel-time and ray-path utilities. Seismol. Res. Lett., 70, 2, 154–160. DOI: 10.1785/gssrl.70.2.1540

DMR: 2007, Geological Map of Thailand. Ministry of Natural Resources and Environment, Thailand.

Ferrari, O.M. Hochard, C. and Stampfli, G.M.: 2007, Contribution to the geology of Thailand and implications for the geodynamic evolution of Southeast Asia. Tectonophysics, 451, 1-4, 346–365. DOI: 10.1016/j.tecto.2007.11.065

Guan, Z. and Niu, F.: 2017, An investigation on slowness-weighted CCP stacking and its application to receiver function imaging. Geophys. Res. Lett., 44, 12, 6030–6038. DOI: 10.1002/2017GL073755

Hansen, B.T. and Wemmer, K.: 2011, Age and evolution of the basement rocks in Thailand. In: Ridd, M.F., Barber, A.J. and Crow, M.J. (eds.), The Geology of Thailand, 1st ed. The Geological Society of London, 19–32. DOI: 10.1144/GOTH.2

Hawkesworth, C.J., Cawood, P.A., Dhuime, B. and Kemp, T.I.S.: 2017, Earth's continental lithosphere through time. Ann. Rev. Earth Planet. Sci., 45, 1, 169–198. DOI: 10.1146/annurev-earth-063016-020525

Hurukawa, N., Tun, P.P. and Shibazaki, B.: 2012, Detailed geometry of the subducting Indian Plate beneath the Burma Plate and subcrustal seismicity in the Burma Plate derived from joint hypocenter relocation. Earth Planets Space, 64, 4, 333–343. DOI: 10.5047/eps.2011.10.011

Katsura, T., Yoneda, A., Yamazaki, D., Yoshino, T. and Ito, E.: 2010, Adiabatic temperature profile in the mantle. Phys. Earth Planet. Inter., 183, 1-2, 212–218. DOI: 10.1016/j.pepi.2010.07.001

Kennett, B.L.N. and Engdahl, E.R.: 1991, Traveltimes for global earthquake location and phase identification. Geophys. J. Int., 105, 2, 429–465. DOI: 10.1111/j.1365-246X.1991.tb06724.x

Knapmeyer-Endrun, B., Kruger, F. and Group TPW: 2014, Moho depth across the Trans-European Suture Zone from P- and S-receiver functions. Geophys. J. Int., 197, 2, 1048–1075. DOI:10.1093/gji/ggu035

Kreemer, C., Blewitt, G. and Klein, E.C.: 2014, A geodetic plate motion and global strain rate model. Geochem. Geophys. Geosyst., 15, 10, 3849–3889. DOI: 10.1002/2014GC005407

Latiff, A.H.A. and Khalil, A.E.: 2019, Crustal thickness and velocity structure of Malay Peninsula inferred from joint inversion of receiver functions and surface waves dispersion. J. Asian Earth Sci., 169, 105–116. DOI: 10.1016/j.jseaes.2018.08.011

Ligorría, J.P. and Ammon, C.J.: 1999, Iterative deconvolution and receiver-function estimation. Bull. Seismol. Soc. Am., 89, 5, 1395–1400. DOI: 10.1785/BSSA0890051395

Liu, H. and Niu, F.: 2012, Estimating crustal seismic anisotropy with a joint analysis of radial and transverse receiver function data: Estimating crustal seismic anisotropy. Geophys. J. Int., 188, 1, 144–164. DOI: 10.1111/j.1365-246X.2011.05249.x

Maurin, T., Masson, F., Rangin, C., Min, U.T. and Collard, P.: 2010, First global positioning system results in northern Myanmar: Constant and localized slip rate along the Sagaing fault. Geology, 38, 7, 591–594. DOI: 10.1130/G30872.1

Minezaki, T., Hisada, K., Hara, H. and Kamata, Y.: 2019, Tectono-stratigraphy of Late Carboniferous to Triassic successions of the Khorat Plateau Basin, Indochina Block, northeastern Thailand: Initiation of the Indosinian Orogeny by collision of the Indochina and South China blocks. J. Asian Earth Sci., 170, 208–224. DOI: 10.1016/j.jseaes.2018.10.020

Morley, C.K., Charusiri, P. and Watkinson, I.M.: 2011, Structural geology of Thailand during the Cenozoic. In: Ridd, M.F., Barber, A.J. and Crow, M.J., (eds.), The Geology of Thailand, 1st ed. The Geological Society of London, 273–334. DOI: 10.1144/GOTH.11

Morley, C.K., Woganan, N., Sankumarn, N., Hoon, T.B., Alief, A. and Simmons, M.: 2001, Late Oligocene–Recent stress evolution in rift basins of northern and central Thailand: Implications for escape tectonics. Tectonophysics, 334, 2, 115–150. DOI: 10.1016/S0040-1951(00)00300-0

Noisagool, S., Boonchaisuk, S., Pornsopin, P. and Siripunvaraporn, W.: 2014, Thailand's crustal properties from tele-seismic receiver function studies. Tectonophysics, 632, 64–75. DOI: 10.1016/j.tecto.2014.06.014

Noisagool, S., Boonchaisuk, S., Pornsopin, P. and Siripunvaraporn, W.: 2016, The regional moment tensor of the 5 May 2014 Chiang Rai earthquake (Mw=6.5), Northern Thailand, with its aftershocks and its implication to the stress and the instability of the Phayao Fault Zone. J. Asian Earth Sci., 127, 231–245. DOI: 10.1016/j.jseaes.2016.06.008

Nwe, L., Wei, Z., Li, Z., Bao, F., Li, X. and Hu, J.: 2022, Crustal thickness, VP/VS ratio, and shear wave velocity structures beneath Myanmar and their tectonic implications. Earthq. Res. Adv., 2, 1, 100060. DOI: 10.1016/j.eqrea.2021.100060

Pananont, P., Herman, M.W., Pornsopin, P., Furlong, K.P., Habangkaem, S., Waldhauser, F. and Wechbunthung, B.: 2017, Seismotectonics of the 2014 Chiang Rai, Thailand, earthquake sequence. J. Geophys. Res., Solid Earth, 122, 8, 6367–6388. DOI: 10.1002/2017jb014085

Rattana, P.: 2020, Stratigraphy and geochemistry of rock salt from Maha Sarakham formation in Changwat Chaiyaphum, northeastern Thailand. Chulalongkorn University. Theses and Dissertations, Bangkok, 35

Ridd, M.F.: 2017, Chapter 16 Karen–Tenasserim unit. Geol. Soc. Lond. Mem., 48, 1, 365–384. DOI: 10.1144/M48.16

Ridd, M.F., Barber, A.J. and Crow, M.J.: 2011, Introduction to the geology of Thailand. In: Ridd, M.F., Barber, A.J. and Crow, M.J., (eds.), The Geology of Thailand, 1st ed. The Geological Society of London, 1–17. DOI: 10.1144/GOTH.1

Saetang, K.: 2017, Focal mechanisms of Mw 6.3 aftershocks from waveform inversions, Phayao Fault Zone, Northern Thailand. Int. J. Geophys. DOI: 10.1155/2017/9059825

Saetang, K.: 2022, Two-layer model of anisotropy beneath Myanmar and Thailand revealed by shear-wave splitting. Ann. Geophys., 65, 6, 1–13. DOI: 10.4401/ag-8769

Saetang, K. and Durrast, H.: 2023, A minimum 1-D velocity model of Northern Thailand. J. Seismol., 27, 493–504. DOI: 10.1007/s10950-023-10148-6

Saetang, K., Srisawat, W. and Durrast, H.: 2018, Crustal structures, geothermal sources and pathways beneath Northern Thailand revealed by local earthquake tomography. Chiang Mai J. Sci., 45, 1, 565–575.

Searle, M.P. and Morley, C.K.: 2011, Tectonic and thermal evolution of Thailand in the regional context of SE Asia. In: Ridd, M.F., Barber, A.J. and Crow, M.J. (eds.,) The Geology of Thailand, 1st ed. The Geological Society of London, 539-571. J. Geol. Soc. Lond. DOI: 10.1144/GOTH.20

Shi, J., Wang, T. and Chen, L.: 2020, Receiver function velocity analysis technique and its application to remove multiples. J. Geophys. Res., Solid Earth, 125, 8, e2020JB019420. DOI: 10.1029/2020JB019420

Simmons, N.A., Forte, A.M., Boschi, L. and Grand, S.P.: 2010, GyPSuM: A joint tomographic model of mantle density and seismic wave speeds. J. Geophys. Res., Solid Earth, 115 B12, 2010JB007631. DOI: 10.1029/2010JB007631

Simons, W.J.F., Socquet, A., Vigny, C. and Ambrosius, B.A.C., Haji Abu, S., Promthong, C., Subarya, C., Sarsito, D.A., Matheussen, S., Morgan, P. and Spakman, W.: 2007, A decade of GPS in southeast Asia: Resolving sundaland motion and boundaries. J. Geophys. Res., Solid Earth, 112, B6, 2005JB003868. DOI: 10.1029/2005JB003868

Singtuen, V., Phajuy, B., Anumart, A., Charusiri, P., Chawthai, N. and Heggemann, H.: 2023, Geochemistry and provenance of Mesozoic sandstones in Khon Kaen Geopark: Implication for tectonics of the western Khorat Plateau of Thailand. PLoS ONe, 18, 4, e0284974. DOI: 10.1371/journal.pone.0284974

Stokes, R.B., Lovatt Smith, P.F. and Soumphonphakdy, K.: 1996, Timing of the Shan-Thai-Indochina collision: New evidence from the Pak Lay Foldbelt of the Lao PDR. Geol. Soc. Lond. Spec. Publ., 106, 1, 225–232. DOI: 10.1144/gsl.sp.1996.106.01.14

Sun, W. and Kennett, B.L.N.: 2020, Common-reflection-point-based prestack depth migration for imaging lithosphere in Python: Application to the dense Warramunga array in northern Australia. Seismol. Res. Lett., 91, 5, 2890–2899. DOI: 10.1785/0220200078

Than, N.M., Khin, K. and Thein, M.: 2017, Chapter 7 Cretaceous geology of Myanmar and Cenozoic geology in the Central Myanmar Basin. Geol. Soc. Lond. Mem., 48, 1, 143–167. DOI: 10.1144/M48.7

UNAVCO: 2021, GPS Velocity Viewer. https://www.unavco.org/software/visualization/GPS-Velocity-Viewer/GPS-Velocity-Viewer.html. Accessed 27 December 2023

Xu, M. and He, J.: 2023, Seispy: Python module for batch calculation and postprocessing of receiver functions. Seismol. Res. Lett., 94, 2A, 935–943. DOI: 10.1785/0220220288

Xue, M., Le, K.P. and Yang, T.: 2013, Seismic anisotropy surrounding South China Sea and its geodynamic implications. Mar. Geophys. Res., 34, 407–429. DOI: 10.1007/s11001-013-9194-4

Yu, Y., Gao, S.S., Liu, K.H., Yang, T., Xue, M., Le, K.P. and Gao, J.: 2018, Characteristics of the mantle flow system beneath the Indochina Peninsula revealed by teleseismic shear wave splitting analysis. Geochem. Geophys. Geosyst., 19, 5, 1519–1532. DOI: 10.1029/2018GC007474

Zhu, L. and Kanamori, H.: 2000, Moho depth variation in southern California from teleseismic receiver functions. J. Geophys. Res., Solid Earth, 105, B2, 2969–2980. DOI: 10.1029/1999JB900322